Atomic Energy Control Board
P.O. Box 1046
Ottawa, Canada
K1P 5S9

Commission de contrôle de l'énergie atomique
C.P. 1046
Ottawa, Canada
K1P 5S9

INFO-0253-1

MICROCOMPUTER BASED PROGRAM FOR PREDICTING HEAT TRANSFER UNDER REACTOR ACCIDENT CONDITIONS
VOLUME I: TEXT

by

S.C. Cheng, D.C. Groeneveld,
L.K.H. Leung, Y.L. Wong, C. Nguyen
University of Ottawa

A research report prepared for the
Atomic Energy Control Board
Ottawa, Canada

Project No. 86.1.19

July 1987

Canada

Research report

MICROCOMPUTER BASED PROGRAM FOR PREDICTING HEAT TRANSFER UNDER REACTOR ACCIDENT CONDITIONS

ABSTRACT

A microcomputer based program called Heat Transfer Prediction Software (HTPS) has been developed. It calculates the heat transfer for tube and bundle geometries for steady state and transient conditions. This program is capable of providing the best estimated of the hot pin temperatures during slow transients for 37- and 28-element CANDU type fuel bundles. The program is designed for an IBM-PC AT/XT (or IBM-PC compatible computer) equipped with a Math Co-processor. The following input parameters are required: pressure, mass flux, hydraulic diameter, and quality. For the steady state case, the critical heat flux (CHF), the critical heat flux temperature, the minimum film boiling temperature, and the minimum film boiling heat flux are the primary outputs. With either the surface heat flux or wall temperature specified, the program determines the heat transfer regime and calculates the surface heat flux, wall temperature and heat transfer coefficient. For the slow transient case, the pressure, mass flux, quality, and volumetric heat generation rate are the time dependent input parameters required to calculate the hot pin sheath temperatures and surface heat fluxes.

A simple routine for generating properties has been developed for light water to support the above program. It contains correlations that have been verified for pressures ranging from 0.6kPa to 30 MPa, and temperatures up to 1100°C. The thermodynamic and transport properties that can be generated from this routine are: density, specific volume, enthalpy, specific heat capacity, conductivity, viscosity, surface tension and Prandtl number for saturated liquid, saturated vapour, subcooled liquid or superheated vapour.

A software for predicting flow regime has also been developed. It determines the flow pattern at specific flow conditions, and provides a correction factor for calculating the CHF during partially stratified horizontal flow.

The technical bases for the program and its structure are discussed. A user's instruction for the HTPS is also included.

RÉSUMÉ

Un programme de micro-ordinateur, appelé Heat Transfer Prediction Software (HTPS) (logiciel de prévision du transfert de la chaleur), a été élaboré. Il calcule le transfert de chaleur pour les configurations de tubes et de grappes dans des conditions de régimes transitoires lents et stationnaires. Le programme peut estimer les températures des aiguilles de combustible chaudes durant les régimes transitoires lents des grappes de combustibles de type CANDU composées de 28 et de 37 éléments. Le programme est conçu pour un ordinateur IBM-PC AT/TX (ou pour un ordinateur compatible avec le IBM-PC) muni d'un coprocesseur mathématique. Les paramètres d'entrées suivants sont nécessaires : pression, flux massique, diamètre hydraulique et qualité. En régime stationnaire, les principales sorties sont le flux thermique critique, la température du flux thermique critique, la température minimale de l'ébullition en film et le flux thermique minimal de l'ébullition en film. Si l'on précise le flux thermique en surface ou la température du mur, le programme détermine le régime de transfert de chaleur et calcule le flux thermique en surface, la température du mur et le coefficient de transfert de chaleur. En cas de transitoire lent, la pression, le flux massique, la qualité et le taux volumétrique de production de chaleur sont les paramètres d'entrée requis pour calculer les températures des gaines des aiguilles et les flux thermiques en surface.

Un sous-programme simple pour créer des propriétés a été élaboré pour l'eau légère afin d'appuyer le progiciel indiqué ci-dessus. Il renferme des corrélations qu'on a vérifié à des pressions qui varient de 0,6 kPa à 30 MPa, et des températures jusqu'à 1100°C. Les propriétés thermodynamiques et de transport que peut produire le sous-programme sont les suivantes : densité, volume spécifique, enthalpie, capacité de chaleur spécifique, conductivité, viscosité, tension superficielle et nombre de Prandtl pour le liquide saturé, vapeur saturée, liquide sous-refroidi ou vapeur surchauffée.

Un logiciel pour prévoir le régime de l'écoulement a aussi été élaboré. Il détermine le régime de l'écoulement dans des conditions de débit spécifiques et il fournit un facteur de correction pour calculer le flux thermique critique durant un débit horizontal partiellement stratifié.

Les fondements techniques du programme et de sa structure sont discutés. Un guide d'instructions du logiciel de prévision du transfert de chaleur est aussi inclus.

DISCLAIMER

The Atomic Energy Control Board is not responsible for the accuracy of the statements made or opinions expressed in this publication and neither the Board nor the author assume liability with respect to any damage or loss incurred as a result of the use made of the information contained in this publication.

FOREWORD

This report consists of two volumes:

Volume 1 contains introduction, heat transfer correlations, two-phase regime flow prediction methods, heat transfer logic, transient analysis of hot pin temperature, evaluation of light water properties, heat transfer prediction software (HTPS) package, HTPS package user's instruction, conclusion, final remarks and recommendations for further work, references, tables and figures.

Volume 2 consists of appendices I through V describing flow regimes in horizontal flow, flow regimes in vertical flow, horizontal CHF prediction method, U.O. property code for light water and HTPS source code.

TABLE OF CONTENT

	Page
ABSTRACT	i
DISCLAIMER	iii
FORWORD	v
NOMENCLATURE	xi
ACKNOWLEDGMENT	xv
LIST OF TABLES	xvii
LIST OF FIGURES	xix

VOLUME I: TEXT

1.	INTRODUCTION	1
2.	HEAT TRANSFER CORRELATIONS	3
	2.1 Boiling Curve	3
	2.2 Forced Convection to Liquid	3
	2.3 Onset of Nucleate Boiling	5
	2.4 Nucleate Boiling and Forced Convective Evaporation	5
	2.5 Critical Heat Flux (CHF) Point	7
	2.6 Transition Boiling	8
	2.7 Minimum Film Boiling Point	9
	2.8 Film Boiling	9
	2.9 Forced Convection to Vapour	12
	2.10 Application of the Prediction Methods to Heavy Water	12
3.	TWO-PHASE REGIME FLOW PREDICTION METHODS	15
	3.1 Flow Regime Map for Horizontal Flow	15
	3.2 Flow Regime Map for Vertical Flow	16
4.	HEAT TRANSFER LOGIC	17
	4.1 Temperature Controlled Mode	17
	4.2 Heat Flux Controlled Mode	18
	4.2.1 CHF = q_{min}	18
	4.2.2 CHF < q_{min}	18
	4.2.3 CHF > q_{min}	19
5.	TRANSIENT ANALYSIS OF HOT PIN TEMPERATURE	21
	5.1 Transient Heat Calculation	21
	5.2 Fuel Properties	22
	5.3 Effect of Flow Stratification on Hot Pin Temperature	23
6.	EVALUATION OF LIGHT WATER PROPERTIES	25
	6.1 First Level	25
	6.2 Second Level	26
	6.3 Third Level	26
7.	HEAT TRANSFER PREDICTION SOFTWARE (HTPS) PACKAGE	29
	7.1 Compilation and Execution	29

7.2 Structure of the HTPS Package 30
7.2.1 Main Program 30
7.2.2 Input and Output Routines 32
7.2.3 Heat Transfer Logic Routines 32
7.2.4 Heat Transfer Correlation Routines 32
7.2.5 Utility Routines 34
7.2.6 Fluid Properties Routines 35
7.2.7 Table Block Data 35

8. HTPS PACKAGE USER'S INSTRUCTION 37
8.1 Description of Keys 37
8.2 HTPS Package Activation 38
8.3 HTPS Input 38
8.4 Between Input and Output 39
8.5 HTPS Output 39

9. CONCLUSIONS 41

10. FINAL REMARKS AND RECOMMENDATIONS FOR FUTURE WORK 44

11. REFERENCES 45

TABLES 49

FIGURES 53

VOLUME II: APPENDICES

I. FLOW REGIMES IN HORIZONTAL FLOW 1
II. FLOW REGIMES IN VERTICAL FLOW 15
III. HORIZONTAL CHF PREDICTION METHOD 27
IV. U.O. PROPERTY CODE FOR LIGHT WATER 35
V. HTPS SOURCE CODE 57
SUBROUTINE LOGO 58
SUBROUTINE BER 62
SUBROUTINE BERSON 65
SUBROUTINE CALCHF 70
SUBROUTINE CALCUX 74
SUBROUTINE CALG 77
SUBROUTINE CONVERT 79
SUBROUTINE EVALUA 82
SUBROUTINE FB 95
SUBROUTINE GRODEL 97
SUBROUTINE GROENE 101
SUBROUTINE HTLOGIC 109
SUBROUTINE INCHOIC 134
SUBROUTINE INSTEAD 140
SUBROUTINE INTRANS 153
SUBROUTINE INTRAN1 164
SUBROUTINE MINFBT 173
SUBROUTINE NB 176

SUBROUTINE OUTSTEA 181
SUBROUTINE OUTTRAN 188
SUBROUTINE RADHF 193
SUBROUTINE SPLFC 194
SUBROUTINE SPSFC 197
SUBROUTINE STEADY 201
SUBROUTINE TB 204
SUBROUTINE TEMP 206
SUBROUTINE TRNSNT 209
REAL FUNCTION HALP 215
REAL FUNCTION INTRP3 216
REAL FUNCTION UCP 220

NOMENCLATURE

Symbol	Definition	Unit
A	flow area	m^2
Bo	boiling number	
C	fuel properties coefficient	
CHF	Critical Heat Flux	$W.m^{-2}$
Cp	specific heat capacity	$J.kg^{-1}.K^{-1}$
D	diameter	m
E	enhancement factor	
Fr	Froude number	
Fr^+	modified Froude number as defined in equation (17)	
f	friction factor	
G	mass flux	$kg.m^{-2}.s^{-1}$
G_1	lower mass flux threshold	$kg.m^{-2}.s^{-1}$
G_2	higher mass flux threshold	$kg.m^{-2}.s^{-1}$
g	acceleration due to gravity	$m.s^{-2}$
H	enthalpy	$J.kg^{-1}$
H_{fg}	latent heat of vaporization	$J.kg^{-1}$
h	heat transfer coefficient	$W.m^{-2}.K^{-1}$
h_L	equilibrium liquid height	m
j	superficial velocity	$m.s^{-1}$
K	CHF correction factor	
K^+	product of modified Froude number and the square root of superficial Reynolds number of liquid as defined in equation (19)	
k	conductivity	$W.m^{-1}.K^{-1}$
l	tube length	m
l_e	entry length for stable slug flow	m
M	molecular weight	$g.mole^{-1}$
Nu	Nusselt number	
P	pressure	KPa,Pa
Pe	Peclet number	
Pr	Prandtl number	
Q	heat content	W
$q_{"}$	heat flux	$W.m^{-2}$
q'''	volumetric heat generation rate	$W.m^{-3}$
R	gas constant	$cal.mole^{-1}$
Re	Reynolds number	
S	suppression factor	
s	perimeter	m
T	temperature	^oC,K
T^+	ratio of turbulent to gravity forces acting on the gas as defined in equation (18)	
TD	theoretical density	$kg.m^{-3}$
t	time	s
U	phase velocity	$m.s^{-1}$
Vol	volume	m^3
X	quality	
X	Martinelli's parameter	

Y	Petukhov's parameter or Taitel and Dukler's parameter	

Greek	Definition	Unit
α	void fraction	
β	porosity coefficient	
γ	inclination angle	
ϵ	emissivity	
μ	viscosity	$kg.m^{-1}.s^{-1}$
φ	Groeneveld-Delorme parameter	
ρ	density	$kg.m^{-3}$
σ	surface tension	$N.m^{-1}$
θ	reference temperature in equation (24)	K

Subscript

a	actual
Ber	Berenson's equation
b	bulk fluid
c	at thermodynamic critical point
CHF	at Critical Heat Flux point
conv	convective boiling
d	at departure of nucleate boiling
e	equilibrium
FB	film boiling
f	saturated liquid
G	vapour phase
GD	Groeneveld-Delorme's correlation
g	saturated vapour
H	homogeneous
h, hor	for horizontal flow
hy	hydraulic equivalent
K	Katto's equation
L	liquid phase
min	at minimum film boiling point
mod	modified
NB	at nucleate boiling
pool	pooling boiling
r	reduced
rad	radiation
SP	at single-phase convection to liquid
sat	at saturation
store	stored
sub	subcooled
TB	at transition boiling
tt	turbulent liquid-turbulent vapour
UO2	uranium dioxide properties
v	vapour
va	actual vapour
ve	equilibrium vapour

ver	for vertical flow
vf	vapour film
w	wall
w-v	wall-to-vapour
8	for 8mm tube

Superscript

*	temperature in degree Kelvin
~	dimensionless parameter

ACKNOWLEDGMENT

The authors would like to thank Mr. R.A. Judd for permitting the use of his screen formatting function routines. His helpful assistance in the course of developing the input/output software is appreciated. The initial setup of the input/output software was performed by Mrs. A. Leung. Her skillful programming technique, which eases the complexity of later modification, is gratefully acknowledged.

The authors also thank the staff of the Atomic Energy Control Board for the helpful discussions and sample listing in developing the logic of transient case.

Funding of this investigation was provided by the Atomic Energy Control Board.

LIST OF TABLES

VOLUME I: TEXT

Table		Page
1.	Critical Heat Flux Look-Up Table	49
2.	CHF Correction Factors	51
3.	Summary of Function Keys	52

VOLUME II: APPENDICES

III.1	G_1/G_2 vs. P and X (D = 0.01 m)	32
III.2	K_6 vs. G and X (P = 10 MPa, D = 0.01 m)	33

LIST OF FIGURES

VOLUME I: TEXT

Figure		Page
1.	Schematic Diagram of a Boiling Curve	53
2.	Regions of Heat Transfer in Convective Boiling	54
3.	Heat Transfer Configuration	55
4.	Effect of Quality on Boiling Curve	56
5.	Effect of Mass Flux and Subcooling on Boiling Curve	57
6.	Boiling Curve for a Heat Flux Controlled System	58
7.	Boiling Curve for a Temperature Controlled System	59
8.	Generalized Flow Regime Map for Horizontal Flow	60
9.	Flow Regime Map for Steam-Water Upward Flow in a 5.1 cm Diameter Tube at 1.0 atm	61
10.	Start-up Stage of the Heat Transfer Logic	62
11.	Heat Transfer Logic for a Temperature Controlled Mode	63
12.	Transition from Single-Phase Forced Convection to Liquid to Nucleate Boiling	64
13.	Heat Transfer Logic for a Heat Flux Controlled Mode (CHF = q_{min})	65
14.	Heat Transfer Logic for a Heat Flux Controlled Mode (CHF < q_{min})	66
15.	Heat Transfer Logic for a Heat Flux Controlled Mode (CHF > q_{min})	67
16(a).	Flowchart for First Level	68
16(b).	Flowchart for Second Level	69
17.	Printout of the General Parameters Input Page	70
18.	Printout of the Steady State Parameters Input Page	70
19.	Printout of the Time Independent Transient Parameters Input Page	71

20.	Printout of the Time Dependent Transient Parameters Input Page	71
21.	Printout of the Steady State Output Page for Unique Heat Transfer Mode	72
22.	Printout of the Steady State Output Page for Multiple Heat Transfer Modes	72
23.	Printout of the Transient State Output Page	73
24.	HTPS Logo Screen	74
25.	HTPS General Parameters Input Screen	74
26.	HTPS Steady State Parameters Input Screen	75
27.	HTPS Transient State Time Independent Parameters Input Screen	75
28.	HTPS Transient State Time Dependent Parameters Input Screen	76
29.	HTPS Executing Message Screen	76
30.	HTPS Finishing Message Screen	77
31.	HTPS Steady State Output Screen for Unique Heat Transfer Mode	77
32.	HTPS Steady State Output Screen for Multiple Heat Transfer Modes	78
33.	HTPS Transient State Output Screen	78

VOLUME II: APPENDICES

I.1	Equilibrium Stratified Flow	9
I.2	Equilibrium Liquid Level for Stratified Flow	9
I.3	Equilibrium Liquid Level for Horizontal Stratified Flow	10
I.4	Flowchart for Subroutine REGH	11
II.1	Flowchart for Subroutine REGV	20
II.2	Flow Patterns in a Vertical Evaporator Tube	21

II.3	Flow Regime Map for Steam-Water Upward Flow in a 5.1 cm Diameter Tube at 10 MPa	22
II.4	Flow Regime Map for Steam-Water Upward Flow in a 1.0 cm Diameter Tube at 10 MPa	23
III.1	Modified Generalized Flow Regime Map for Horizontal Flow	34

1. INTRODUCTION

Fuel sheath temperatures in water-cooled nuclear reactors are near the saturation temperature of water. However, during an accidental increase in power, or a decrease in flow and pressure, deterioration in heat transfer is possible. This occurs when the surface temperature increases to such a high level that the heated surface can no longer support continuous liquid contact. This phenomenon is referred to as the boiling crisis or dryout, and the corresponding heat flux as the critical heat flux or CHF. The boiling crisis is characterized by either a sudden rise in surface temperature, caused by the heated surface being covered by a stable vapour film (film boiling), or by small surface temperature spikes, corresponding to the appearance and disappearance of dry patches (transition boiling).

Due to the poor vapour heat transfer properties, high surface temperatures are often encountered in the post-CHF or post-dryout region. Although nuclear reactors normally operate under conditions where dryout does not occur, prevention of dryout during accidents is not always possible. One of the postulated accidents is a loss of coolant accident (LOCA), caused by a rupture in the primary coolant system. Accurate prediction of the consequences of a LOCA requires precise calculation of fuel-coolant heat transfer during (1) the blowdown phase (when the fuel channel is voided), and (2) the subsequent emergency-core-cooling (ECC) phase. A variety of prediction methods is currently used in accident analysis.

Heat transfer modes encountered during a LOCA or any other incident where the fuel dries out, depend on the fuel sheath temperature. The boiling curve (Figure 1) illustrates this departure for a given set of flow conditions (note that the shape of the boiling curve during flow boiling is similar, but not identical to the pool boiling curve). Along the length of a heated channel the flow conditions, especially the fluid enthalpy, will change. The resulting change in heat transfer mode is illustrated in Figure 2 [1].

In the literature, a variety of heat transfer correlations has been recommended for each heat transfer mode. Common heat transfer configurations encountered in reactor components are shown in Figure 3 [2]. The choice of heat transfer correlation depends on the following main factors: geometry of heat transfer surface, orientation of the surface, direction of the flow, and local phase distribution.

Phase distribution is the most significant factor especially at low flow in horizontal channels. The pattern of phase distribution can be determined through flow regime maps or from comparison to the flow regime boundary criteria for simple geometries (details are described in Chapter 3). For complex

geometries such as rod bundle, experimental results indicate that the flow regime boundaries shift slightly from those for a simple geometry. Despite these differences, the prediction using the flow regime for simple geometry would provide useful information for subchannel analysis of bundle geometry.

Due to the complexity of the heat transfer mechanisms, an empirical approach is often necessary. For each heat transfer mode there are numerous empirical correlations available, and each correlation is only valid for a narrow range of conditions. A better approach is to derive a single heat transfer correlation based on suitably defined local parameters (e.g., X, D_{hy}, α) to characterize the heat transfer process.

Evaluation of the heat transfer correlations requires the knowledge of the thermodynamic and transport properties of fluids. The accuracy of these properties affects strongly the performance of the adopted correlations. Fluid properties are available in various means: tables, correlations, software for mainframes and for microcomputers. The employment of properties tables is rather troublesome and will slow down the evaluation process significantly. Utilizing computer software routines is a simple and accurate method to obtain fluid properties especially for large number of calculation. Some of the software routines are, however, proprietary and therefore unavailable in general use. This prompts a need of developing properties routine codes.

Boiling heat transfer is complex, and requires cumbersome mathematical expressions for heat transfer correlations. The use of mainframe computers can significantly simplify the process, however, there are problems regarding high cost and accessibility to mainframe computers. Because of the widespread use of microcomputers in engineering evaluation of thermalhydraulic processes, there is a need for a microcomputer-based software package for evaluating heat transfer.

In the present work, the microcomputer based Heat Transfer Prediction Software (HTPS) package is developed based on the generalized heat transfer correlations which are considered to be valid for reactor accident conditions. Also, a program is developed to predict flow regimes for vertical and horizontal flows.

2. HEAT TRANSFER CORRELATIONS

2.1 Boiling Curve

In a heated channel, with subcooled liquid at the inlet, the following heat transfer regimes will be encountered sequentially as illustrated in Figure 2:

i) forced convection to liquid
ii) nucleate boiling
iii) transition boiling
iv) film boiling
v) forced convection to vapour.

Note that nucleate boiling changes into forced convective evaporation at high qualities, and transition boiling may not be encountered in a heat flux controlled system.

These heat transfer regimes occur for a gradually increasing enthalpy or vapour quality. Although useful for illustrating the change in heat transfer, Figure 2 cannot be used for determining which type of heat transfer regime is present. This requires knowledge of the boiling curve shown schematically in Figure 1. Although the shape of the boiling curve changes slightly with a change in pressure, mass flux, enthalpy, and geometry, the basic relationship between the individual heat transfer regimes remains unaltered. Figure 4 [2A] shows the detailed effect of a change in quality on the boiling curve, the effects of other parameters are presented in Figure 5. Various heat transfer regimes are separated from each other by transition points. The most important ones are located between nucleate boiling and transition boiling (CHF point: T_{CHF}, CHF) and between transition boiling and film boiling (minimum film boiling point: T_{min}, q_{min}). These are indicated as points 1 and 2, respectively in Figure 1. The remaining transition point located between forced convection to liquid and nucleate boiling (onset of nucleate boiling point) is less important since the transition is gradual.

The following sections describe the recommended prediction methods for each of the heat transfer modes and transition points.

2.2 Forced Convection to Liquid

In power reactor systems, a commonly encountered mode of energy exchange between fuel and coolant is single-phase heat transfer, e.g. water-cooled reactors, upstream from the point of onset of nucleate boiling. In addition, the heat transfer in nuclear steam generators and preheater is due to, in part, single-phase heat transfer. The prediction of the single-phase

heat transfer coefficient for tube geometry was significantly improved by the Dittus & Boelter correlation [3] which can be expressed as

$$Nu = 0.023\ Re^{0.8}\ Pr^{0.4} \qquad (1)$$

After the Dittus-Boelter equation, many correlations have been presented; most of them have the same form but differ in the coefficient and/or the exponent values. The difference in these values suggest that constant values may not be capable of covering a wide range of conditions. Recently, Petukhov [4] has developed an analytical equation for predicting heat transfer in a circular tube with uniform wall heat flux. To account for the variable properties, an empirical ratio of viscosities has been introduced to satisfy the experimental data for heating and cooling with uniform wall temperature. In reference [5] Petukhov equation for tubes is expressed as

$$Nu = 0.125\ f\ Re\ Pr\ Y^{-1}\ (\mu_b/\mu_w)^n \qquad (2)$$

where

$$Y = 1.07 + 12.7\ (Pr^{2/3} - 1)\ (0.125\ f)^{0.5} \qquad (2a)$$

$$f = (1.82 \log Re - 1.64)^{-2} \text{ (for smooth surfaces)} \qquad (2b)$$

$$n = \begin{cases} 0.11 & \text{heating with uniform } T_w \quad (T_w > T_b) \\ 0.25 & \text{cooling with uniform } T_w \quad (T_w < T_b) \\ 0 & \text{uniform wall heat flux or gases} \end{cases}$$

The correlation was derived using the averaged energy, momentum, and continuity equations, and is applicable to smooth tubes. For a rough surface, equation (2b) has to be replaced by the Colebrook & White equation. The Petukhov equation is the most up-to-date correlation and has been verified against a wide range of experimental data. Good agreement has been obtained with data in the range of

$$10^4 < Re < 5 \times 10^6$$
$$0.5 < Pr < 2000$$
$$0.08 < \mu_w/\mu_b < 40$$

Tube correlations may be applied to other geometries as well, provided that the Reynolds number is evaluated based on the hydraulic diameter concept. Some difficulties in using the hydraulic diameter concept have been encountered [6], but they only appear in cross sections with sharp corners. Since the flow channel of the CANDU bundles do not consist of sharp corner (except for the spacers and bearing pads regions), a tube correlation together with the hydraulic diameter would provide a reasonable approximation.

2.3 Onset of Nucleate Boiling

The point at which the first bubble is generated (Figure 2) is referred to as the Onset of Nucleate Boiling (ONB) point. It is used to signify the transition from single-phase to two-phase. Some of the bubbles formed after this point might leave the wall, however, these detached bubbles only travel a short distance before condensing in the bulk fluid. In general, the ONB point can be determined using empirical correlations which are valid only for a limited range. Extrapolation outside the range is usually not recommended. In the present software package, a simple method that consistently provides the expected trend is adopted. It involves the evaluation of the wall temperatures (or heat fluxes) for both the single-phase liquid convection and the nucleate boiling regions. These two calculated wall temperatures (or heat fluxes) are then compared with each other to determine the heat transfer regime (Figure 12). The detailed discussion of this method is presented in sections 4.2 and 4.3.

2.4 Nucleate Boiling and Forced Convective Evaporation

Nucleate boiling is the most efficient heat transfer mode in equipment operated with a two-phase mixture. The transition between single-phase liquid convection and nucleate boiling is called partial nucleate boiling, in which single-phase liquid convection and nucleate boiling are equally important. However, this intermediate regime can be ignored since the errors involved have been found to be negligible.

Many pre-CHF boiling heat transfer prediction methods have been developed either in the form of correlations or a graphical methods. Among these, Shah's [7] and Chen's [8] correlations have frequently been recommended. Recently, Gungor & Winterton [9] presented a prediction method which has a wider range of validity. Their equations are expressed as follows:

$$h_{tp} = E\, h_{conv} + S\, h_{pool} \tag{3}$$

where

$$h_{conv} = 0.023\, Re_f^{0.8}\, Pr_f^{0.4}\, k_f/D \tag{3a}$$

$$h_{pool} = 55\, P_r^{0.12}\, (-\log_{10} P_r)^{-0.55}\, M^{-0.5}\, q^{0.67} \tag{3b}$$

$$E = 1 + 24000\, Bo^{1.16} + 1.37\, (1/X_{tt})^{0.86} \tag{3c}$$

$$S = (1 + 1.15\times10^{-6}\, E^2\, Re_f^{1.17})^{-1} \tag{3d}$$

$$P_r = P/P_c \tag{3e}$$

$$X_{tt} = (1/X_a - 1)^{0.9} (\rho_g/\rho_f)^{0.5} (\mu_f/\mu_g)^{0.1} \tag{3f}$$

If the channel is horizontal and the Froude number is less than

0.05, the coefficients E and S must be multiplied by

$$E_h = Fr^{(0.1-2Fr)} \qquad (3g)$$

and

$$S_h = Fr^{0.5} \qquad (3h)$$

respectively.

Similar to Chen's correlations, Gungor & Winterton correlation (equation 3) consists of two parts: a pool boiling term with a suppression factor (S) and a forced convection contribution with an enhancement factor (E). The enhancement factor and the suppression factor were developed from a large number of data for various fluids covering the range of

pressure	:	0.08	- 70.12	bar
mass flux	:	12.4	- 8179.3	$kg.m^{-2}.s^{-1}$
diameter	:	2.95	- 32.	mm
quality	:	0.0	- 99.3	%
subcooling	:	0.1	- 173.	K (for subcooled condition)
heat flux	:	0.35	- 2280.	$kW.m^{-2}$

Equation (3) above was tested against experimental data and was found to be more accurate and applicable over a wider range when compared to several other correlations (including Shah's and Chen's correlations) [9,10]. Since the correlation includes a single-phase heat transfer term (h_{conv} in equation 3) as in Chen's correlation, it is valid for both the forced convective evaporation and the nucleate boiling regions.

The calculation of X_{tt} in equation (3f) is based on the actual quality which is the same as the equilibrium quality in an equilibrium system. Under non-equilibrium conditions such as subcooled boiling, the actual and the equilibrium qualities are significantly different. In the present software package, the equilibrium quality is one of the input parameters and the actual quality is calculated from Levy equation [11] as

$$X_a = X_e - X_{e,d} \exp(X_e/X_{e,d} - 1) \qquad (3i)$$

where

$$X_{e,d} = -0.0022 [q D Cp_g / (k_f H_{fg})] \quad \text{for Pe < 70000} \qquad (3j)$$
$$X_{e,d} = -154 Bo \quad \text{for Pe > 70000} \qquad (3k)$$

The above prediction method may be applied to bundle geometries because nucleate boiling is only a local phenomenon and therefore is not significantly dependent on the channel cross section.

2.5 Critical Heat Flux (CHF) Point

The maximum nucleate boiling heat flux is referred to as the critical heat flux. Many CHF correlations (over 400 as of 1982) have been proposed for water. Most of them are valid only within a narrow range of application and provide incorrect asymptotic trend outside the range. Recently, Groeneveld et al. [12] have developed the CHF table look-up approach which provides CHF values for discrete values of pressure (P), mass flux (G), and quality (X) covering the ranges of 0.1-20 MPa, 0-7500 $kg.m^{-2}.s^{-1}$ and -50 to 100% for the above parameters respectively. (The negative qualities refer to subcooled conditions). Linear interpolation is carried out for P, G, and X values not tabulated in the tables. Extrapolation is usually not needed as the tables cover a wide enough range of conditions. Comparison with other correlations and for a wide range of data has indicated that this method is more superior [13]. The CHF tables are shown in Table 1.

The CHF tables are valid only for vertical upward flow inside a uniformly heated 8mm tube, for other condition correction factors are required. For horizontal flow, CHF is affected strongly by flow stratification. This effect could be quite significant at low flows. Groeneveld [14] suggested modifications to the above CHF table look-up method for predicting CHF in horizontal flow. A correction factor based on the mass flux thresholds, which are obtainable from Taitel & Dukler flow regime boundary criteria [15,16], was proposed. Details of the derivation of this stratification factor, K_6, is described in Appendix III.

In addition to the stratification factor K_6 discussed above, several other correction factors have been presented to predict CHF for other configurations. These have been discussed by Groeneveld [14] and are summarized in Table 2.

The modified CHF value is expressed as

$$CHF_a = CHF_8(P,G,X).K_1.K_2.K_3.K_4.K_5.K_6 \qquad (4)$$

where $CHF_8(P,G,X)$ is the value obtained from the CHF tables (Table 1).

The corresponding temperature (T_{CHF}) is obtained from

$$\Delta T_{CHF} = T_{CHF} - T_{sat} = CHF / h_{NB} \qquad (5)$$

where h_{NB} can be obtained as described in section 2.4
T_{sat}: saturated temperature
CHF : from equation (4).

2.6 Transition Boiling

Transition boiling is a unique heat transfer mode where the heat transfer coefficient generally decreases rapidly as the wall temperature increases. It is basically a combination of unstable film boiling and unstable nucleate boiling alternately existing at any given location on a heated surface. Its occurrence depends mainly on the system parameter, i.e. whether the process is heat flux controlled or temperature controlled. In a heat flux controlled system, the temperature increases rapidly from the critical heat flux temperature to the film boiling temperature as shown in Figure 6. As a consequence, the transition boiling regime can hardly be detected. In a temperature controlled system, transition boiling is encountered as the temperature falls within the bounds of critical heat flux temperature and minimum film boiling temperature (Figure 7).

Several correlations have been proposed from experimental studies. They were generally obtained through best fitting of the data; hence, they are valid only over a limited range of conditions and may not provide correct asymptotic trend outside this range. Another approach [2] was developed from the obtained parametric trends and employed linear interpolation between the maximum and the minimum points on a log-log plot of q vs ΔT_w, i.e.

$$\frac{q_{TB}}{q_{min}} = \left(\frac{CHF}{q_{min}}\right)^m \quad \text{where} \quad m = \frac{\ln (\Delta T_{min}/\Delta T_w)}{\ln (\Delta T_{min}/\Delta T_{CHF})} \tag{6a}$$

or

$$\frac{\Delta T_w}{\Delta T_{min}} = \left(\frac{\Delta T_{CHF}}{\Delta T_{min}}\right)^n \quad \text{where} \quad n = \frac{\ln (q_{TB}/q_{min})}{\ln (CHF/q_{min})} \tag{6b}$$

CHF and ΔT_{CHF} are evaluated as shown in section 2.5. The correlation for ΔT_{min} is given in the next section while q_{min} is calculated from

$$q_{min} = \Delta T_{min}\, h_{FB} \tag{7}$$

where h_{FB} can be evaluated as shown in section 2.8.

This prediction method is universal: it provides the correct parametric as well as asymptotic trends. However, because it requires the knowledge of both the critical heat flux and the minimum film boiling points (points 1 & 2 on Figure 1), its applicability depends strongly on the validity of the correlations for these two points.

2.7 Minimum Film Boiling Point

The minimum film boiling point separates the high temperature region (where inefficient film boiling takes place) from the lower temperature region (where the more efficient transition boiling occurs). It thus provides a limit to the application of transition boiling and film boiling correlations. Knowledge of the minimum film boiling temperature is particularly important in nuclear reactor safety assessment.

Because of the different types of film boiling formation and the scarcity of reliable data, not much confidence can be put into any correlation for predicting the minimum film boiling temperature; except perhaps the Groeneveld-Stewart correlation [17], which is expressed as

$$T_{min} = 284.7 + 0.441\ P - 3.72\times10^{-6}P^2 - \mathrm{Max}[0,\ X_e\times10^4\times(2.82 + 0.00122\ P)^{-1}] \qquad (8a)$$

for $P < 9000$ kPa;

$$T_{min} = \Delta T_{min,9000kPa}\ (P_c - P)/(P_c - 9000) + T_{sat} \qquad (8b)$$

for $P > 9000$ kPa. The reasons for this exception are (i) the agreement of this correlation with the data provided by most researchers, and (ii) the correct asymptotic trend of pressure and subcooling. The ranges of applicability for the Groeneveld-Stewart correlation are:

pressure	: 100 - 9000 kPa
mass flux	: 50 - 4000 $kg.m^{-2}.s^{-1}$
quality	: -19 - 64 %
geometry	: vertical upflow in circular tube

Since film boiling is a local wall phenomenon,it is unlikely to be affected by the cross-sectional geometry (except perhaps in very narrow gaps). Hence the suggested correlation is expected to be valid for a wide range of geometries.

The minimum film boiling heat flux can be calculated using the above minimum film boiling temperature and the film boiling correlation (section 2.8).

2.8 Film Boiling

Film boiling is the least efficient heat transfer mode. Here, cooling of the heated surface relies on heat transfer by radiation, by vapour convection, by liquid droplet interaction with the surface, and by conduction. The conduction component is usually negligible due to poor vapour conductivity. The vapour

can become highly superheated; its temperature is controlled both by wall-vapour and vapour-liquid heat exchange. Film boiling models have been developed through the semi-theoretical approach with the interfacial heat and momentum transfer obtained with empirical correlations.

In the empirical approach, the film boiling correlations may be divided into:

a) thermal equilibrium correlation,
b) empirical correlation, and
c) phenomenological correlation.

The thermal equilibrium correlation assumes that the liquid and vapour are in equilibrium, i.e., $X_a = X_e$. This assumption is valid only

i) at high mass flows and high void fractions where the liquid-vapour heat exchange is efficient, or
ii) near the dryout location where the vapour has insufficient time to become superheated.

The empirical correlations generally predict a heat transfer coefficient which is based on the temperature difference between the wall and the saturation condition. They are simple to use but should not be extrapolated outside their recommended range.

The phenomenological correlations are based on the physical mechanisms governing this type of heat transfer and use h_{w-v} based on the vapour temperature. In general, these correlations provide significant improvement over the empirical film boiling correlations. Some of them give correct asymptotic trends to permit smooth convergence toward the single-phase superheated steam cooling equation.

Comparison with the experimental data has indicated that the phenomenological correlations are the most accurate. However, they are generally more complex and difficult to apply. In the present package, the Groeneveld-Delorme correlation [18] is used:

$$h_{GD} = 0.008348(k_{vf}/D)(Re_{vf}[X_a+(1-X_a)(\rho_v/\rho_f)])^{0.8774}Pr^{0.6112} \quad (9)$$

where ρ_v is the vapour density at T_{va}, vapour film properties are evaluated with the vapour film temperature

$$T_{vf} = 0.5\ (T_{va} + T_w) \quad (9a)$$

The actual vapour temperature is obtained from the actual vapour enthalpy which is calculated from

$$H_{va} = H_{ve} + H_{fg}\ \exp(-\tan\phi) \quad (9b)$$

where

$$\phi = 0.13864\ Pr_g^{0.2031}\{Re_g[X_e+(1-X_e)(\rho_g/\rho_f)]\}^{0.2006} (q\ D\ Cp_g/k_g/H_{fg})^{-0.09232}(1.3072-1.0833X_e+0.8955X_e^2) \quad (9c)$$

with $\phi = 0$ for $\phi < 0$, $\phi = \phi$ for $0 < \phi < \pi/2$, and $\phi = \pi/2$ for $\phi > \pi/2$. The Groeneveld & Delorme correlation is recommended because it is valid for a wide range of conditions. This correlation, however, underpredicts the power for the case just above the critical channel powers. It also underpredicts the heat transfer at low pressure, low mass flux, and subcooled conditions. Under these conditions, better prediction can be obtained using Berenson's equation [19], together with the voidage and the subcooling modifications. The modified Bererson equation [20] is presented as

$$h_{Ber} = 0.425\ [k_{vf}^3 g^{1.5} \rho_{vf}(\rho_f-\rho_{vf})^{1.5}(H_{vf}-H_f)]^{0.25} (\mu_{vf}\Delta T_{sat}\ \sigma^{0.5})^{-0.25} \quad (10a)$$

$$h_{mod,Ber} = h_{Ber}\ (1 + 25.5\ \Delta T_{sub} / T_b^*)\ (1 - \alpha_H)^2 \quad (10b)$$

where T_b^* is the bulk fluid temperature in degree Kelvin.

Void fraction is usually predicted from empirical correlations. Due to the high wall temperature in the film boiling regime, actual void measurements are difficult to perform. In the derivation of equation (10b), the homogeneous void fraction equation

$$\alpha_H = [1 + (1-X)\ \rho_g\ /\ (\rho_f X)]^{-1} \quad (11)$$

has been used. This equation, in fact, is applicable for the dispersed film boiling regime, in which the liquid droplets travel at velocities close to the bulk vapour velocity.

The method proposed here is the selection of the maximum heat transfer (or the minimum wall temperature) of the Groeneveld-Delorme correlation (equation 9) and the modified Berenson's equations (10a & b), i.e.

$$h_{FB} = Max\ [h_{GD},\ h_{mod,Ber}] \quad (12a)$$

or

$$T_{FB} = Min\ [T_{GD},\ T_{mod,Ber}] \quad (12b)$$

This prediction method has been compared with a wide range of tube film boiling data and improvement in accuracy has been shown over the use of Groeneveld-Delorme correlation alone. In addition, the method provides the correct asymptotic trend and a gradual change in wall temperature.

Strictly speaking, the proposed prediction method is valid

only for directly heated tubes. Extension to bundle geometry requires some modification. In CANDU type bundle, it has been observed that the post-dryout heat transfer coefficient is considerably higher than that predicted with a fully developed heat transfer coefficient equation (equation 12a) at powers slightly above dryout power. At powers greater than 16% of the dryout power, the heat transfer coefficient converges to the one obtained from equation (12a). Hence, the employment of this prediction method without any modification is a reasonable approach for CANDU type fuel bundle geometries.

At high sheath temperatures, radiation heat transfer becomes significant. Several methods can be used to evaluate the radiation heat transfer. The simplest one is the two gray planes method, which assumes a continuous cylindrical liquid core and gray surface for both the wall and the liquid. Other methods are usually more complicated and require the knowledge of parameters such as absorptivity, and transmissivity of vapour. These parameters are not well known for high pressure steam. Hence, the simple two gray planes method, which is written as

$$q_{rad} = 5.67 \times 10^{-8} \, (T_w^4 - T_{sat}^4) \, (1/\epsilon_w + 1/\epsilon_f - 1)^{-1} \qquad (13)$$

is adopted in the present package.

2.9 Forced Convection to Vapour

Most of the film boiling correlations for tubes are based on the Hadaller superheated vapour equation [21]. The correlations are valid for film boiling, superheated vapour and the transition in between. Thus, an additional equation for the heat transfer by forced convection to vapour is not necessary. For the sake of simplicity and minimizing computing time, the Hadaller superheated vapour equation is directly used once the equilibrium quality is higher than unity. It is written as

$$Nu = 0.008348 \, Re_v^{0.8774} \, Pr_v^{0.6112} \qquad (14)$$

Two correction factors have been proposed to extend the applicability of the above equation to bundle geometry [18]. They are adopted to compensate for the temperature variant around the circumference of the fuel elements due to the poor heat transfer in the gap between two elements. In the present application (i.e. for 28- and 37-element CANDU type bundles), they can probably be neglected since the values are close to unity.

2.10 Application of the Prediction Methods to Heavy Water

The prediction methods for CHF, T_{min} and h_{FB} are based on

light water data only. They may be applied to heavy water conditions provided the dimensional parameters be replaced by suitable dimensionless groups. This approach has been used to determine the critical heat flux in the CHF table method [22, 23]. The parameters have been non-dimensionalized with pressure replaced by ρ_f/ρ_g, mass flux by $G\ D^{0.5}\ \sigma^{-0.5}\ \rho_f^{-0.5}$ (as suggested by Katto & Ohno [24]) and CHF by $CHF/G.H_{fg}$. This dimensionless approach of using the CHF table has been tested extensively for six different fluids and was found to provide better CHF predictions than any other multi-fluid CHF prediction method [22, 23].

The film boiling prediction method (section 2.8) is already in terms of dimensionless groups and does not require any further modifications. The correlation for the minimum film boiling temperature has been made dimensionless by using reduced properties, i.e. by replacing all pressures and temperatures by P/P_c and T/T_c. The correlation in its dimensionless form thus becomes

$$\frac{T_{min}^*}{T_c^*} = 0.862+1.5071\frac{P}{P_c} - 2.8122\left(\frac{P}{P_c}\right)^2 + \frac{Max\ [0, -X]}{0.1825+1.747P/P_c} \qquad (15a)$$

for $P/P_c < 0.407$ and

$$\frac{T_{min}^*}{T_c^*} = \frac{T^*_{min,0.407}}{T_c^*}\ \frac{(1 - P/P_c)}{0.593} + \frac{T_{sat}^*}{T_c^*} \qquad (15b)$$

for $P/P_c \geq 0.407$.

Since the differences between D_2O and H_2O properties are small, the correlation derived for H_2O can be applied to D_2O with insignificant loss of accuracy.

3. TWO-PHASE FLOW REGIME PREDICTION METHODS

Prediction of two-phase thermalhydraulic quantities such as void fraction, pressure drop and heat transfer requires the knowledge of phase distribution. Taitel and Dukler [15] have developed schemes for determining the flow regime in both vertical and horizontal flows. Based on their work, two computer subroutines REGH and REGV have been written for flow regime determinations in horizontal and vertical flow, respectively. The following sections present the use of flow-regime maps in both horizontal and vertical flows. The detailed development and description of the two subroutines are given in Appendices I and II.

3.1 Flow Regime Map for Horizontal Flow

Taitel and Dukler [15] have developed a mechanistic model for predicting the transition between flow regimes in horizontal tube flow. Due to the generalized nature of the map, their method is widely used.

Figure 8 shows the generalized flow regime map for horizontal flow based on Taitel and Dukler's work where the coordinates are expressed as follows:

x-axis

$$X = \left(\frac{1-X}{X}\right)^{0.9}\left(\frac{\mu_f}{\mu_g}\right)^{0.1}\left(\frac{\rho_g}{\rho_f}\right)^{0.5} \tag{16}$$

y-axis

$$Fr^{+} = \frac{GX}{(\rho_g(\rho_f-\rho_g)D_{hy}g)^{0.5}} \tag{17}$$

$$T^{+} = \left[\frac{0.092G^{1.8}(1-X)^{1.8}\mu_f^{0.2}}{gD_{hy}^{1.2}\rho_f(\rho_f-\rho_g)}\right]^{0.5} \tag{18}$$

$$K^{+} = \left[\frac{G^3X^2(1-X)}{\rho_g(\rho_f-\rho_g)\mu_f g}\right]^{0.5} \tag{19}$$

For given flow conditions (G,X,P,D), X as well as Fr^{+}, T^{+} and K^{+} can be calculated. With this information, the user can locate the point on the flow regime map. It should be noted that multiple scales are used in this generalized flow regime map. When locating the point, care must be taken to ensure the correct position by referring to the correct scale. The procedure for locating the correct flow regime is:

i) Check to see if the point (Fr^+,$\underline{X}$) is above or below curve A.

ii) If the point is below curve A go to step iii) otherwise, check to see if the value of $\underline{X}$ is less or greater than 1.6. If $\underline{X}$ is less than 1.6,the flow regime is annular. If $\underline{X}$ is greater than 1.6,check the point (T^+,$\underline{X}$) to see if it is above or below curve D. The flow regime is intermittent if the point is below curve D and dispersed bubbly if the point is above curve D.

iii) Check the location (K^+,$\underline{X}$) against curve C. If it is above curve C, the flow regime is stratified wavy otherwise, it is stratified smooth.

The horizontal flow regime map can be used for determining the correction factor for horizontal CHF, K_6, as described in Appendix III.

3.2 Flow Regime Map for Vertical Flow

Taitel and Dukler [16] analyzed the transitions between different flow patterns based on their model. The flow pattern map thus created (Figure 9) has simple coordinates(j_f and j_g) and there is little ambiguity involved in the various transitions. This figure created for a 5.1cm diameter tube with steam-water at 1 atm.

To determine the flow regime, the values of j_f and j_g are first evaluated where

$$j_f = G\ (1 - X)/\rho_f \tag{20}$$

and

$$j_g = G\ X/\rho_g \tag{21}$$

Using Figure 9, a point can be located with the corresponding flow regime determined. If the point falls in the slug-churn region, additional information - the tube length (l) is required. If the point of observation is 100 diameters downstream of the entrance, then one uses the curve l_ϵ/D_{hy}=100 as the transition boundary between slug and churn flow. If l is not given, no distinction will be made between slug and churn flow; instead, they will loosely be classified as slug-churn regime.

4. HEAT TRANSFER LOGIC

Heat Transfer logic is an event sequence in determining the heat transfer mode for a specific set of conditions. The logic follows basically the boiling curve (Figure 1) for a specific set of parameters (i.e. pressure, mass flux, diameter and quality). It proceeds firstly by locating the two major transition points: the departure of nucleate boiling (DNB or CHF) point, and the minimum film boiling point (points 1 & 2 of Figure 1, respectively). The specified heat flux or wall temperature is then compared with the respective values at the transition points to determine the heat transfer regime. Figure 10 shows the flow diagram for the start-up stage of the heat transfer logic. The procedure for determining the heat transfer regimes depends upon whether it is heat flux or temperature controlled. The details are discussed in the following sections.

4.1 Temperature Controlled Mode

Components such as steam generator tubes or fuel elements experiencing fast transients are usually considered to behave in a temperature controlled mode. The process to determine the heat transfer regime or transition point for a temperature controlled situation is straightforward. It is illustrated in Figure 11 and described schematically as follows:

$T_{CHF} < T_w < T_{min}$ ----> Transition Boiling

$T_w > T_{min}$ ----> Film Boiling or
Forced Convection to Vapour

$T_w < T_{CHF}$ ----> Nucleate Boiling or
Forced Convection to Liquid

To distinguish between film boiling and vapour cooling, a comparison based on quality is made:

$X_a < 1$ ----> Film Boiling

$X_a > 1$ ----> Vapour Cooling

As the actual quality X_a is usually unknown, the equilibrium quality X_e may be used to obtain an approximate value. The distinction between film boiling and vapour cooling may not be necessary since frequently the same correlation may cover both ranges.

To distinguish between single-phase convection to liquid and nucleate boiling (including forced convective evaporation at high qualities) the approach of evaluating the onset of nucleate boiling (ONB) point is often used. For most applications, this approach may be simplified by comparing the wall temperature to

those at the two transition points. That is,

$T < T_{sat}$ ----> Single Phase Convection to Liquid

$T_{sat} < T < T_{CHF}$ and $q_{SP} > q_{NB}$ ----> Single Phase Convection to Liquid

$T_{sat} < T < T_{CHF}$ and $q_{SP} < q_{NB}$ ----> Nucleate Boiling

The logic for determining these two heat transfer regimes is shown in Figure 12.

4.2 Heat Flux Controlled Mode

Electrically or nuclear heated elements during steady state conditions behaves in a heat flux controlled mode. The determination of the heat transfer for a heat flux controlled mode is more complex than for a temperature controlled mode as more than one heat transfer regimes can occur for the same heat flux. The flow diagrams of the heat transfer logic are shown in Figure 13-15.

4.2.1 CHF = q_{min}

This is frequently the assumed case in a heat flux controlled mode. As the heat flux reaches the critical heat flux point (maximum point), the temperature increases rapidly from T_{CHF} to film boiling temperature. Transition boiling region is either not present or occurred so fast that detection is not possible. The flow diagram for this case (Figure 13) shows that

$q < CHF$ and $T_{w,SP} < T_{w,NB}$ ----> Single Phase Convection to Liquid

$q < CHF$ and $T_{w,SP} > T_{w,NB}$ ----> Nucleate Boiling (or Forced Convective Evaporation)

$q > CHF$ ----> Film Boiling

4.2.2 CHF < q_{min}

This case is encountered at high flows and/or high qualities where the boiling curve does not display a minimum as was shown in Figure 3. This corresponds to a gradually increasing T_w, when the heat flux is slowly increased above the CHF. Figure 14

illustrates the logic diagram for this case. It is basically similar to the above case (CHF = q_{min}) except for q > CHF where the following heat transfer regimes are possible:

CHF < q < q_{min} ----> Transition Boiling

q > q_{min} ----> Film Boiling

4.2.3 CHF > q_{min}

This case corresponds to a boiling curve having both a maximum and minimum as shown in Figure 1 and hence more than one heat transfer regime can be encountered if the heat flux falls between the CHF and q_{min}. For q > CHF or q < q_{min} the heat transfer logic remains unchanged from that of section 4.2.1. Note that here the transition boiling is a highly unstable heat transfer regime since a slight reduction in heat flux would result in a shift to the stable film boiling regime, while a slight increase in heat flux would result in a shift to the nucleate boiling regime. Figure 15 shows the logic for this case and the three possible heat transfer regimes are indicated for q_{min} < q < CHF.

5. TRANSIENT ANALYSIS OF HOT PIN TEMPERATURE

Nuclear reactors operate normally under conditions such that the total generated heat is carried away by the coolant which is at or below the saturation temperature. During a Loss-of-Coolant Accident (LOCA) and subsequent Emergency Core Cooling (ECC), because of the degradation in the flow conditions, the fuel would experience a temperature excursion which may be quite severe for cases where the loss of the coolant is accompanied by a power pulse. Analytical tools are currently available for analyzing this accident scenario. For example, computer code FIREBIRD, developed by Atomic Energy of Canada Limited - Candu Operations, has been used to calculate the hot pin temperatures. Because of its complexity, this code is expensive to run. There is a need therefore to develop a simpler and less expensive method for the purpose of scoping studies.

This chapter describes the development of such prediction method to give the best estimate of the hot pin sheath temperature transient for a horizontal CANDU type fuel bundle. The hot pin refers to the top fuel element of the horizontal bundle. This element usually experiences dryout first due to flow stratification. Unlike the steady state (in which all generated heat is transferred to the coolant), the heat removed by the coolant can be less than the generated heat. The remaining heat inside the fuel element, called the stored heat, causes the fuel temperature to increase. The calculation of the stored heat requires the knowledge of the fuel element diameter which is also an input parameter in the transient prediction. Other than the fuel element diameter and the bundle hydraulic equivalent diameter (which are constant throughout the time step), the local parameters such as pressure, mass flux, quality, and volumetric heat generation rate are required as a function of time. In return, the input local parameters as well as the calculated surface heat flux and sheath temperature are tabulated at each time step.

It should be noted that, since a lumped parameter approach is adopted, the present package is valid only for relatively slow transients.

5.1 Transient Heat Calculation

The generated heat (q'''.volume) may be divided into two parts. One part is carried away by the coolant (convective heat) while the remaining part is used to heat up the fuel element (stored heat). The convective heat is calculated by

$$Q_{conv} = h\ A\ (T_w - T_b) \qquad (22)$$

where T_b, the bulk fluid temperature, is assumed to be equal to

the saturation temperature for all boiling heat transfer modes. The heat transfer mode is selected using the logic described in Chapter 4. Subsequently, h is evaluated using the steady state correlations in Chapter 2.

An exact evaluation of the fuel temperature-time transient, in general, involves a complex numerical analysis. To simplify the process, a lumped parameter approach is adopted. Assuming a uniform temperature across the fuel element, the fuel temperature transient can be obtained when the decay heat generation rate is provided. It is expressed in the form of

$$\begin{aligned} Q_{store} &= q'''.Vol - Q_{conv} \\ &= \rho_{UO2}\ C_{PUO2}\ Vol\ (\delta T_w/\delta t) \end{aligned} \qquad (23)$$

The effect of this assumption of uniform temperature across the fuel element on the fuel sheath temperature transient would be insignificant provided the temperature profile inside the fuel element does not change significantly during the total time period.

5.2 Fuel Properties

The evaluation of the fuel temperature transient depends strongly on the accuracy of the fuel properties. Since there are no published fuel properties data or correlations for fuel under operating conditions, the unirradiated fuel properties are used. Tong & Weisman [25] have presented expressions and values for various fuel properties. A constant value of 10970 $kg.m^{-3}$ is used for the density of UO_2. The expression for the specific heat capacity of UO_2 is taken from the MATPRO fuel handbook [26]. It is written as

$$\begin{aligned} C_{PUO2} = 15.496\ (T^{-2}\ [C_1\theta^2 \exp(\theta/T)]\ [\exp(\theta/T) - 1]^{-1} + 2\ C_2 T \\ + C_3\ C_4\ \exp(-C_4/RT)\ /\ (RT^2)\ ) \end{aligned} \qquad (24)$$

where

C_{PUO2}	= specific heat capacity	$(J.kg^{-1}.K^{-1})$
C_1	= 19.145	$(cal.mol^{-1}.K^{-1})$
C_2	= 7.8473×10^{-4}	$(cal.mol^{-1}.K^{-2})$
C_3	= 5.6437×10^{6}	$(cal.mol^{-1})$
C_4	= 37694.6	$(cal.mol^{-1})$
θ	= 535.285	(K)
T	= temperature	(K)
R	= 1.987	$(cal.mol^{-1}.K^{-1})$

Considerable amount of research has been performed to obtain the thermal conductivity for unirradiated UO_2. Correlations have been proposed through best fitting the data for different

temperature ranges [26]. They are written as

$$k_{UO2} = [1-\beta(1-TD)][1-0.05\beta]^{-1}[C_5/(C_6+T)+C_7\exp(C_8T)] \quad (25a)$$

for $0^oC < T \leq 1650^oC$, and

$$k_{UO2} = [1-\beta(1-TD)][1-0.05\beta]^{-1}[C_9+C_7\exp(C_8T)] \quad (25b)$$

for $1650^oC < T \leq 2840^oC$. The coefficients and parameters are defined as

k_{UO2} = thermal conductivity ($W.cm^{-1}.K^{-1}$)
TD = fraction of theoretical density (= 0.95 is assumed)

β = porosity coefficient ($= 2.58 - 0.58\times10^{-3}T$)
T = temperature (^oC)
C_5 = 40.4
C_6 = 464
C_7 = 1.216×10^{-4}
C_8 = 1.867×10^{-3}
C_9 = 0.0191

5.3 Effect of Flow Stratification on Hot Pin Temperature

Prediction for the hot pin heat transfer depends strongly upon the occurrence of flow stratification. It is assumed that at time = 0 (the first time step), steady state conditions are present (i.e. all generated heat is transferred to the coolant). The surface heat flux is evaluated from the volumetric heat generation rate and the wall temperature is determined using the steady-state heat transfer logic as described in Chapter 4.

For the subsequent time step, the initial surface heat flux is assumed to be the same as the final heat flux calculated from the previous time step. The mass flux thresholds for flow stratification are evaluated from the flow regime boundary equations (Appendix III), and are compared with the input mass flux. If the input mass flux is larger than the upper threshold value (G_2), flow stratification is assumed not to occur. The wall temperature is simply calculated from the steady-state heat transfer logic. If the input mass flux is less than the lower threshold value (G_1), complete flow stratification is assumed. For an input mass flux between the two thresholds ($G_1 < G < G_2$), the flow is partially stratified. The correction factor for CHF is calculated and applied. The heat transfer is evaluated with the steady-state logic since the hot element is partly wetted by the coolant. If complete flow stratification is present ($G < G_1$), the top fuel element is most likely located in the vapour region. The heat transfer is then predicted assuming cooling with superheated steam. It is assumed that the liquid-vapour inter-

face transfer can be neglected. The mass flow of vapour is calculated from the vapour mass fraction, X, and the total mass flow. By neglecting the liquid entrainment, the vapour area is computed with the homogeneous void fraction equation described in section 2.8. Using the lumped parameter approach, the stored heat in the fuel pin is determined with the calculated wall temperature (section 5.1). The combined stored and convective heat flux term is compared with the input heat generation. If the difference is more than 2% of the input heat generation, an iterative procedure is carried out until convergence is achieved.

6. EVALUATION OF LIGHT WATER PROPERTIES

There are several computer codes available to calculate light water properties, e.g. STPH and POLSAW (AECL proprietary). However, these codes were written mainly for the mainframe. In light of the availability of low cost micros, there is a need to develop a new property code for such application. University of Ottawa has undertaken such a task and developed a new code - U.O. code, with due consideration of the limited memory size and slow execution time associated with micros. The U.O. code is being used in our current efforts to develop a microcomputer based heat transfer prediction method suitable for reactor accident conditions, and the code is called from subroutine PROPER.

The U.O. code was written in Fortran and uses simple correlations to calculate the properties. The calculated properties are specific volume (V), enthalpy (H), specific heat (CP), viscosity (VIS), thermal conductivity (K) and surface tension (ST). The required input parameters are pressure (P), temperature (T) and selection of types of properties (SEL).

The U.O. code is divided into three different levels as shown in Figure 16. First level represents the main subroutine which determines the phase of fluid and calls appropriate property subroutines from the second level. Second level contains property subroutines which in turn calls certain functions from the third level for calculating water properties. All property equations except that of surface tension are contained at the third level. More detailed description of the U.O. code is presented in Appendix IV along with its nomenclature.

6.1 First Level

The main subroutine is called H2O (residing in subroutine PROPER) which allows the main program to call at any time whenever estimation of properties is required. The passing parameters for this subroutine - pressure in Pa, temperature in C and selection (SEL) - are located in common block AAA. SEL is one dimensional integer array with six elements for selecting properties desired, e.g., set SEL(1) = 1 for specific volume, SEL(2) = 1 for enthalpy ... SEL(6) = 1 for surface tension. If some properties are not desired then set the corresponding elements to 0.

To determine the phase of a fluid, the saturated temperature (TS) has to be calculated first via

$$TS = A + \frac{B}{\log(10^{-6}P) + C} - 273.15 \qquad (26)$$

note P is expressed in Pa.
According to the difference between TS and T, there are three possibilities, i.e.,

|TS - T|	≤	0.001TS	---->	saturated
TS	>	T	---->	subcooled
TS	<	T	---->	superheated

The phase of the fluid is then assigned under the name of PHASE as subcooled, saturated or superheated, and is located inside common block REGIME.

Based on SEL, one or more property subroutines at the second level will be called. Further depending on PHASE, a particular property function at the third level will be called to calculate the property. All calculated properties are stored in common block OUTH2O. For a saturated state, the properties both at saturated liquid and vapour will be predicted.

6.2 Second Level

At this level, there are six property subroutines as cited below.

SUBVOL(TS, VF, VG)	for specific volume
SUBENT(TS, HF, HG)	for enthalpy
SUBCP (TS, CPF, CPG)	for specific heat
SUBVIS(TS, VISF, VISG, VG)	for viscosity
SUBK (TS, KF, KG, VG)	for thermal conductivity
SUBST (TS, ST)	for surface tension

where F and G appearance after the property name representing subcooled or saturated liquid, and saturated or superheated vapour, respectively. In this code, the specific volume for subcooled liquid is approximated via the saturated liquid at the same temperature.

In addition to the passing parameters as shown in the argument of subroutines, there are also pressure and temperature in common block AAA and the phase of fluid in common block REGIME. The calculated values of properties are transferred back to the main calling program under variable names in subroutines.

6.3 Third Level

There are fifteen real functions at this level to calculate a particular water property for a given phase. These are:

FNCVF(T)	specific volume for saturated liquid
FNCVG(T,P)	specific volume for saturated vapour

FNCVG2(T,TS,P)	specific volume for superheated vapour
FNCHF2(T,P)	enthalpy for subcooled liquid
FNCHF(T)	enthalpy for saturated liquid
FNCHG(T)	enthalpy for saturated vapour
FNCHG2(T,TS,P)	enthalpy for superheated vapour

FNCPF2(T,P), FNCPF(T), FNCPG(T) and FNCPG2(T,TS,P) for specific heat

FNCVIF(T,P)	viscosity for subcooled or saturated liquid
FNCVIG(T,VG,I)	viscosity for saturated vapour (I=2) or superheated vapour (I=1)

FNCKF(T,P) and FNCKG(T,VG) for thermal conductivity

The function for surface tension is listed directly under SUBST subroutine at second level.

The U.O. code is valid for temperatures from the triple point (0.01^{o}C) to 1100^{o}C and pressures from 611.3 Pa to 30 MPa. Based on the results of 6000 data points, it can be concluded that, in general, predictions for all properties have an rms error of less than 3% with some exceptions such as near the critical point or specific heat near the saturated state.

The programing size for U.O. code including roughly 150 constants used for the correlations is about 19 kilobytes (k), after compiling it requires 23 k. The execution time of U.O. code is also compared favorably with existing codes. One added feature of U.O. code is its flexibility. For example, if the phase is known or predetermined, to calculate a specific property, one can simply call the third level directly anywhere in the program by writing, for example

```
VF = FNCVF(T)
```

where VF is the specific volume for saturated liquid.

7. HEAT TRANSFER PREDICTION SOFTWARE (HTPS) PACKAGE

The HTPS package contains subroutines for various correlation for different heat transfer regimes as well as those for calculating the transition points. The program is written in Fortran V which is the most widely used high level computer language in engineering applications. Because of high computing cost in utilizing mainframe computers and the widespread use of microcomputers, this prediction method is designed for an IBM-PC AT/XT or other compatible microcomputers. In addition to the cost saving, the microcomputer can also provide the advantage of full screen interactive editing. This advantage can ease the modification of input data, and hence, reduces time consumption.

7.1 Compilation and Execution

The Fortran source code has to be compiled to the machine language so that the computer can execute a series of instructions. For an IBM-PC AT/XT micro-computer, two Fortran compilers are available: MICROSOFT Fortran Compiler and Professional Fortran Compiler. These two compilers have been compared and the Professional Fortran Compiler is found to be more compatible to the Fortran compiler installed in the mainframe computer. The Professional Fortran Compiler requires less executing time since it uses a Math Co-processor (which is part of the required hardware for this compiler). The need for a Math Co-processor represents some disadvantage of this compiler because the overhead cost is increased and the flexibility is reduced (this means that only those IBM-PC AT/XT or compatible micro-computers equipped with a Math Co-processor can execute the compiled software). Since the co-processor would probably become one of the standard features in microcomputers, this disadvantage will diminish in the near future.

Compilation of the Fortran program is a rather long and lengthy process. The large source code is divided into small modules which are compiled individually. Modification to any sub-program requires only the re-compilation of the modified routines, as a result, the compilation time can significantly be reduced. After the compilation process, an object file is created for each sub-program. All object files required in the code have to be linked. The linking process generates an executable code which can be executed to provide the solution for designated problems.

The overall view of transforming the Fortran source code into an executable form has been presented briefly above. The prime necessary hardware for the present package is the IBM-PC AT/XT or compatible microcomputers equipped with the Math Co-processor. The necessary software is the executable HTPS package. If there is a need to modify the HTPS package, the

Fortran source code together with the object files, the Professional Fortran Compiler, and the IBM-PC Linker are required. Details regarding the compiling of the Fortran code and the linking of the object codes can be found in the Professional Fortran Compiler Reference Manual [27].

7.2 Structure of The HTPS Package

The structure of the HTPS package can be divided into seven blocks:

1. main program,
2. input and output routines,
3. heat transfer logic routines,
4. heat transfer correlation routines,
5. utility routines,
6. fluid properties routines, and
7. table data blocks.

The variables used in each routine are transferred through the argument list of the call statement or the common blocks. The source codes for all the sub-programs are attached in Appendix V. The following sections describe most of the sub-programs in the present package.

7.2.1 Main Program

The purpose of the main program is the linking of major subroutines. Hence, no mathematical calculation is involved.

7.2.2 Input and Output Routines

The input and output subroutines receive the input parameters from the user interactively, and present the solutions on the screen. Some of the utility functions used to format the screen are developed by R.A. Judd of the Atomic Energy of Canada Limited.

Modification on the input values can easily be performed within the same page. With the help of screen formatting functions, the cursor keys are activated and any input area corresponding to a particular input value can be located. A legitimate input value, however, is required in the current location before the cursor is allowed to move on to another one. In addition to the cursor keys, other keys can also be defined for specific functions. The <RETURN> key is assigned to move the cursor to the next input area. The <ESC> key is the indication for terminating the program. The <Ctrl-End> signifies the completion of current input page.

In the present package, there are six subroutines for handling the input and output parameters. The first input routine (INCHOIC) is designated for the general input parameters such as unit, fluid type, geometry, orientation, and state of the system. A copy of the input page is shown in Figure 17 to illustrate the setup and the valid choices in each parameter.

The second input routine (INSTEAD) is used to obtain the steady state input data of pressure, mass flux, hydraulic equivalent diameter, quality (or bulk fluid temperature in subcooled liquid and superheated steam conditions), and either heat flux or wall temperature. The input page for this routine is shown in Figure 18. If both the heat flux and the wall temperature are unknown, the prediction package can still provide part of the results when other parameters are given.

The third input routine (INTRAN1) is written to gather the time independent input for transient calculation. These input values include fuel pin diameter, hydraulic equivalent diameter, and flow area. The setup of this page is similar to the routine INSTEAD and is shown in Figure 19.

The last input routine (INTRANS) is developed to handle the time dependent transient input data including time, pressure, mass flux, quality, and volumetric heat generation rate. The input page, which is shown in Figure 20, is arranged in tabulated form. Due to the assumption of steady state as the initial stage, 0 second is set to be the first time step. All the input data are set up as arrays in the program. The size of these arrays is declared to be 100 which is the total number of time steps that can be accommodated. It can be modified by simply changing the number to any desirable value in the present package.

The first output routine (OUTSTEA) is used to present the steady state results. The standard output includes the critical heat flux, the critical heat flux temperature, the minimum film boiling temperature, and the minimum film boiling heat flux. Other output consists of either one or three set(s) of heat transfer regime(s), surface heat flux(es), wall temperature(s) and heat transfer coefficient(s). The printouts of this output page are shown in Figure 21 for single result of heat transfer regime and in Figure 22 for multiple results of heat transfer regimes.

The second output routine (OUTTRAN), which is shown in Figure 23, is written to print out the transient state results. It has similar form as that of the input routine (INTRANS). The input parameters together with the calculated surface heat flux and sheath temperature are listed as a function of time.

7.2.3 Heat Transfer Logic Routines

The heat transfer logic routines are written based on the logic presented in Chapter 4. The input/output parameters are transferred through the call statement or the common blocks. Calculations are performed by calling the heat transfer correlation subroutines. Comparison of the input heat flux or wall temperature to the corresponding values at the two transition points is carried out to determine the heat transfer regime. Specific heat transfer correlation subroutine is called to evaluate the heat transfer results.

The subroutine HTLOGIC is designed to accept the general parameters from INCHOIC and call the respective subroutine depending on the state (steady or transient) of the system. It also has the capability to start the process again, if required.

The subroutine STEADY is written to perform the calculation of the steady state results. It calls the routine INSTEAD to get the input parameters such as pressure, mass flux, etc. (section 7.2.2) and the routine EVALUA to compute the heat transfer results. The results are then displayed on the screen by the routine OUTSTEA.

The subroutine TRNSNT is developed for the evaluation of heat transfer in slow transient. The time independent input parameters are obtained by calling the routine INTRAN1, while the time dependent input variables are gathered from INTRANS. The evaluating process involves some calculations in this subroutine and the calling of routine EVALUA. The computed output will be listed via the routine OUTTRAN.

The subroutine EVALUA can be referred to as the brain of the package. It evaluates the critical heat flux, the critical heat flux temperature, the minimum film boiling temperature, and the minimum film boiling heat flux by calling the respective subroutines. If either the heat flux or wall temperature is provided, it performs the comparison of the input value to the respective values in the two transition points and determines the heat transfer regime. The corresponding subroutine is then called to calculate the results.

7.2.4 Heat Transfer Correlations Routines

Input and output parameters are transferred through the CALL statement or the common blocks. Depending upon whether the heat flux or the wall temperature is known, an iteration technique may be employed to evaluate the results.

The Petukhov correlation (equation 2) is adopted for single-phase liquid forced convection and is incorporated into the subroutine SPLFC. The equation is ready to use with prescribed wall temperature. In case of prescribed heat flux, the wall temperature is determined through iterations.

The Gungor & Winterton equations (equation 3) are used for both nucleate boiling and forced convective evaporation. The equations are organized in the subroutine NB. The heat transfer coefficient is based on the saturated fluid properties. Because the surface heat flux is one of the parameters in the heat transfer coefficient for pool boiling, an iterative technique is required when the wall temperature is prescribed.

The critical heat flux (CHF) is obtained using the table look-up method presented by Groeneveld et al. [12]. The discrete values of pressure, mass flux, quality and CHF are organized in arrays. CHF values for conditions in between the table values of pressure, mass flux, and quality are located by linear interpolation. The evaluation procedure is installed in the subroutine CALCHF and the interpolation procedure is put in two functions (INTRP and INTRP2). For flow of heavy water, the routine CONVERT is used to convert the input data to light water equivalent data. These light water equivalent values are employed to evaluate the CHF which is then converted to the CHF for heavy water. The critical heat flux temperature is calculated by calling the nucleate boiling routine NB.

In horizontal flow, critical heat flux is affected by flow stratification. The occurrence of flow stratification is determined by comparing the input mass flux with the mass flux thresholds (Appendix III). The procedure for finding the mass flux thresholds is arranged in the routine CALG. It also uses an linear interpolating method which is located in the functions (INTRP3 and INTRP). The table data (Table III.1) are obtained from the stability criterion for stratified flow proposed by Taitel and Dukler. For bundle geometry, the threshold values are modified to better fit the data.

The linear interpolation method is adopted in the transition boiling calculation. It is installed in the routine TB. The log of both the wall temperature and the heat flux at the two transition points are calculated and used in the technique.

The minimum film boiling temperature is obtained from the routine MINFBT. It is calculated with the Groeneveld & Stewart correlation (equation 8). The minimum film boiling heat flux is calculated with the routine FB.

Two correlations are involved in the film boiling prediction method, which is located in the routine FB. Subroutine FB is used to compare the heat transfer results obtained by calling the

routines that contain the correlation. The maximum heat transfer coefficient or the minimum wall temperature between the results obtained from the two correlations is adopted.

The Groeneveld & Delorme correlation (equation 9) is organized in the routine GROENE. It contains two sections: one is for the known wall temperature case and the other is for the known heat flux case. Since the correlation requires both the heat flux and the wall temperature, an iterative technique is used in both sections. Computation is more complicated for the known heat flux case, in which the correlation is put in a separate routine GRODEL.

The modified Berenson equation (equation 10) is arranged in the subroutine BERSON. Similar to the routine GROENE, BERSON consists of a section for the known heat flux case and another for the known temperature case. An iterative technique is required only for the known heat flux case of which the equation is organized in the routine BER.

The radiation heat transfer is calculated with the simple two gray planes method (equation 13). The method has been installed in the routine RADHF. It calculates the heat flux due to radiation with an input wall temperature.

The Hadaller superheated steam cooling equation (equation 14) is used for the single-phase convection to vapour and is organized in the subroutine SPSFC. For a given wall temperature, the heat transfer coefficient can be evaluated simply. For a given heat flux, however, iteration is required to obtain the result.

7.2.5 Utility Routines

The utility routines consist of the input/output page setup functions, the supporting correlations, the interpolating technique, the fuel properties, the conversion from temperature to quality and vice versa.

The input/output page setup functions are proprietary materials and are stored in three object codes: BIOSINT, SCWIND, and UTILS. The applications of some functions (lists of input/output in the calling statement) are available, but the details are unable to provide.

The supporting correlations include the function for calculating the homogeneous void fraction (HALP) and the subroutine for converting the heavy water data to the light water equivalent values (CONVERT). The routine HALP is a simple routine that calculates the void fraction with given quality, liquid and vapour densities. The routine CONVERT converts the

heavy water input values to light water equivalent values. It also provides the scaling factor to convert calculated light water equivalent heat flux to heavy water value.

The interpolating technique is stored in the function INTRP and is used in the calculation of critical heat flux and mass flux threshold values. The setup for calling the function INTRP are arranged in the functions INTRP2 and INTRP3, respectively.

The fuel properties involved are density, specific heat and conductivity. The recommended density is a constant value for the temperature range. The specific heat capacity is expressed in a single equation which is installed in the function UCP. The calculation of conductivity is separated as an individual function (UK).

In subcooled or superheated conditions, the quality can be obtained from the enthalpy ratio with the bulk fluid temperature. The calculation is performed in the routine CALCUX. Also, the fluid temperature can be evaluated from the quality. The procedure is developed in the routine TEMP which employs an iterative technique to find the temperature.

7.2.6 Fluid Properties Routines

The fluid properties are obtained from the routines PROPER for light water and PROPD2O for heavy water. They are transferred through the common block PROP and include density, enthalpy, conductivity, viscosity, surface tension, specific heat capacity, specific volume, and Prandtl number of liquid phase, vapour phase, and subcooled or superheated fluid (if required). They also include saturation pressure, saturation temperature, latent heat of vaporization as well as surface tension. The details of light water properties routine are presented in Chapter 6 and Appendix IV.

7.2.7 Table Block Data

These block data routines contain the table values for evaluating the critical heat flux and the flow stratification mass flux threshold. For critical heat flux calculation, the tables include different pressure, mass flux, and quality values. CHF's values at various intervals of these values are also arranged. For mass flux threshold calculation, the tables include different pressure and quality values, and the mass flux threshold at various intervals of these values.

8. HTPS PACKAGE USER'S INSTRUCTION

The Heat Transfer Prediction Software (HTPS) package is developed to be user-friendly. All input and output are performed in a menu-driven mode. The user is free to move around the input area for making necessary changes.

8.1 Description of Keys

The valid keys for each input are fixed. The program will not continue if the input is an invalid character. A BEEP sound is used as an indication for an invalid character. For example: the input of UNIT has the valid input of either 'S' or 'B'. Any character other than these two is invalid. Occasionally, when the user is prompted with the message "Any key to continue", any key is valid in that particular case. For numeric input, the valid keys are ' ', '-', '.', '1', '2', '3', '4,' '5', '6', '7', '8', '9', '0'.

Two major function keys involved in this program are the <ESC> and the <Ctrl-End> keys. The <ESC> key is the master termination key which stops and exits the program normally at any input point. The <Ctrl-End> key is the page completion key which checks the input values and leaves the present page if all input values are valid.

The cursor keys provide the movement around the input areas within the same page. The common ones are the <↑> and the <↓> keys, which control cursor movement to the above or the below input area. Once the cursor reaches the top of the input area, it will remain in that location. The input of <↑> key is ignored and a BEEP will be heard to alert the user. Similarly, the cursor will not go further down when the <↓> key is pressed at the bottom of the input area. The other two cursor keys are utilized only for the input in the transient case. The ←→ key directs the cursor to the left input area of the present one, while the ←→ key takes the cursor to the right input area. If the cursor reaches the left-most (or right-most) input area in the same line of the present one, the cursor goes to the right-most input area of the previous line (or left-most input area of the next line) if the ←→ (or ←→) key is pressed.

The <Return> key is the general input key that moves the cursor to the next input area. In steady state, it is the same as the <↓> key. In transient state, it performs similar action as the ←→ key. A summary of the function keys is shown in Table 3.

8.2 HTPS Package Activation

The Heat Transfer Prediction Software (HTPS) package is activated by typing HTPS (provided the file HTPS.EXE is installed in the correct disc drive). Since the package is rather large, it takes a little bit more time to load. After the loading, the logo page (illustrated in Figure 24) is displayed on the screen to indicate the start of the program. With any key entered, the logo page disappears and the general parameters input routine is activated.

8.3 HTPS Input

The general parameter input page is shown in Figure 25 and is designed to gather five parameters (unit, fluid, etc.). Each parameter is provided with two choices. The default value will appear in each input area. After completing the input, the <Ctrl-End> key is used for leaving the present page. Depending on the STATE of the system, either the steady state input or the transient state input will be needed in the next page.

The steady state input page is shown in Figure 26 and is designed to obtain four basic and one optional input parameters. There are no default value assigned to these parameters and input values are required for the basic parameters. These parameters, however, have been restricted to a limited range of values to avoid invalid input data. The ranges of parameters are :

$$
\begin{aligned}
88 &< P < 20000; \text{ kPa} \\
10 &< G < 10000; \text{ kg.m}^{-2}\text{.s}^{-1} \\
0.002 &< D < 0.1 \text{ ; m} \\
-0.5 &< X < 3 \\
10 &< T < 1500 \text{ ; }^{o}\text{C} \\
0 &< q < 99999; \text{ kW.m}^{-2}
\end{aligned}
$$

For the first three parameters (pressure, mass flux, diameter), the input are rigid. The quality input, however, has some flexibility. If it is unknown (hit the <RETURN> key), bulk fluid temperature input is accepted in subcooled or superheated condition. The heat flux and the wall temperature are the optional input parameters which are flexible. The user can input either the heat flux, the wall temperature, or neither one. Hitting the <RETURN> key causes toggle between heat flux and wall temperature input. The <Ctrl-End> key causes the exit of the input page and the start of the evaluation.

The first transient state input page (shown in Figure 27) has the same form as the steady state input page. It is used to gather three time independent parameters which have no assigned default value and are restricted in limited ranges. The ranges of data are:

$0.002 < D < 0.1$; m
$0.00001 < A < 0.008$; m^2

Enter the <Ctrl-End> key to leave the present page and activate the next input page.

The second transient state input page is shown in Figure 28 and is used to obtain five sets of time dependent parameters which are arranged in table. No default values have been assigned to these parameters and limited ranges are provided. The ranges of data are:

$0 < t < 1000$; sec
$88 < P < 20000$; kPa
$30 < G < 10000$; $kg.m^{-2}.s^{-1}$
$-0.5 < X_{m'} < 3$
$0 < q''' < 999999$; $kW.m^{-3}$

The user is free to move around the input area that contains valid values for making changes. There are, however, two restrictions in this page. The first one is that the first time step has to be 0. This agrees with the assumption of steady state as the initial stage. The second one is that all input values at the same time step are required once the time step has been entered (unless that particular time is blanked out). This is in accord that all input values are necessary to perform the evaluation at each time. The calculation will start once the <Ctrl-End> key is pressed.

8.4 Between Input and Output

Both the beginning and the end of the heat transfer evaluation are indicated with a message page. Figure 29 is the page for the beginning while Figure 30 is the page for the end of the process. The user is asked to input any key at the end of the process to signify that he/she is ready to view the output page. In case of unforseen error occurs, the execution can be terminated by entering the BREAK (<Ctrl-Scroll Lock>) key.

8.5 HTPS output

The output for the steady state case consists of two pages for different situations. The first page is arranged for a unique heat transfer regime solution (illustrated in Figure 31). The second page is designed for multiple heat transfer regimes result (shown in Figure 32). Either one of the two pages is listed. At the bottom of the page, the user is asked whether the next case is required. A negative answer terminates the program normally. A positive answer raises another question regarding the input data. An input of 'M' is for retaining the same set of

data with possible modification. An input of 'I' is for re-initializing the numeric data set and for putting in a new set of data. With the input of 'K', the same results will be listed again.

The output page for the transient state case has the similar form as the input page (Figure 33). Two more columns are provided for the calculated sheath temperature and surface heat flux. In each page, results for 20 time steps are listed. For input that consists of more than 20 time steps, a message will appear at the bottom of the page to ask the user to enter any key when ready for the next page.

** NOTE **

The previous output page will be lost if the new page is requested. A hard copy can be obtained (by entering <Shift-PrtSc>) using a printer so that all results can be viewed at the same time. Another way to read the previous page again is to answer 'Y' when the question of "Next Case?" comes up and enter 'K' for the next question to re-list the output.

After all results have been listed, the same questions as those asked in the steady state case will be displayed.

9. CONCLUSIONS

A software package has been developed to predict the steady state heat transfer for tube and bundle geometries. This package is also capable of evaluating the best estimated sheath temperature for 28- and 37-element CANDU type bundles for slow transients. The prediction scheme follows basically the boiling curve for a specific set of parameters and employs recommended correlations for each heat transfer regime.

In steady state, pressure, mass flux, hydraulic diameter, and quality (or bulk fluid temperature in subcooled and superheated conditions) are the basic input values. Critical heat flux, critical heat flux temperature, minimum film boiling heat flux, and minimum film boiling temperature are calculated and printed out. The surface heat flux and the wall temperature are the optional input values. If either one is specified, the heat transfer regime is determined and the heat flux, the wall temperature and the heat transfer coefficient are calculated.

For slow transients, fuel element diameter, channel hydraulic diameter, and flow area and the time transients of pressure, mass flux, quality, and volumetric heat generation are required to calculate the sheath temperatures as well as the surface heat fluxes.

The software is organized in a user-friendly form for the IBM-PC AT/XT (or other IBM-PC compatible microcomputers) equipped with a Math Co-processor. Input and output are menu-driven and are arranged in pages. The user is free to move around the input area to change the input values. The output are also listed in pages but the user cannot access the data area.

A properties evaluation subroutine for light water has been developed to support the prediction package. It provides the following thermodynamic and transport properties: density, specific volume, enthalpy, specific heat capacity, conductivity, viscosity, surface tension and Prandtl number for saturated liquid, saturated vapour as well as subcooled liquid and superheated vapour.

In addition, a flow regime prediction program has also been developed for both vertical and horizontal flows in simple geometries. The program is used to identify the flow pattern at specific conditions and provide the CHF correction factor for permitting the evaluation of CHF during partially stratified horizontal flow.

10. FINAL REMARKS AND RECOMMENDATION FOR FUTURE WORK

1. Caution should be exercised in extrapolating the current thermodynamic and transport properties to high temperature as the light water properties routine is only valid up to 1100°C. At higher temperatures, steam will dissociate and this will result in significant changes in the fluid properties.

2. The current void fraction model assumes homogeneous two-phase flow, i.e. no slip. It is expected that at low pressures the slip will be significant thus resulting in a higher vapour velocity than predicted with the homogeneous model. This will result in an improved vapour cooling and hence lower hot pin temperature for fully stratified flow.

3. Film boiling heat transfer for fuel bundles is evaluated with the correlation developed for a tube. The extension of the tube correlation has been shown to be valid for high power (i.e. power > 116% dryout power). However, the sheath temperature is over-predicted when power lies between the dryout power and 116% dryout power. Studies can be performed to develop a correction factor for the film boiling correlation to improve the prediction in that region.

4. The present prediction method is designed for flow boiling. For conditions such as a large break in the primary circuit or after emergency core cooling, the flow might travel slowly or, in the worst case, become stagnant. Different correlations may be needed for these conditions (extremely low flow and stagnant fluid), and some modifications are required to the HTPS package.

5. The current prediction of the temperature-time transient is based on the assumption of a uniform fuel temperature across the fuel element. For a fast transient case an improvement can be made by solving the 1-D transient conduction equation thus allowing more accurate calculation of Q_{store} component. The Zircaloy sheath, the fuel (UO_2) and the gap in between the fuel and sheath will be modelled as multiple layers. The conduction heat transfer will be calculated with local properties for each layer.

11. REFERENCES

1. Collier, J.G., Convective Boiling and Condensation, 2nd Edition, McGraw-Hill, New York, 1981.

2. Groeneveld, D.C. and Snoek, C.W., A Comprehensive Examination of Heat Transfer Correlation Suitable for Reactor Safety Analysis, Multiphase Science and Technology, Vol. 2, 1986.

2A. Groeneveld, D.C. and Rousseau,J.C., CHF and Post-CHF Heat Transfer: An Assessment of Prediction Methods and Recommendations for Reactor Safety Codes, Advance in Two-Phase Flow and Heat Transfer, Editors: S.C.Kakac/M.D.Ishii, Vol.1, PP. 203-238, Martinus Nijhoff Publisher, 1983.

3. Dittus, F.W. and Boelter, L.M.K., Heat Transfer in Automobile Predictions of the Tubular Type, University of California Publications, Vol. 2, pp. 443-461, 1930.

4. Petukhov, B.S., Heat Transfer and Friction in Turbulent Pipe Flow with Variable Physical Properties, Advances in Heat Transfer, Academic, New York, pp. 504-564, 1970.

5. Ozisik, M.N., Heat Transfer: A Basic Approach, McGraw-Hill, 1985.

6. Irvine, T.R., Noncircular Convective Heat Transfer, Modern Developments in Heat Transfer, Academic, New York, 1963.

7. Shah, M.M., Chart Correlation for a Saturated Boiling Heat Transfer: Equation and Further Study, ASHRAE Transaction, Vol.88, Part 1, pp. 185-196, 1982.

8. Chen, J.C., A correlation for Boiling Heat Transfer to Saturated Fluids in Convective Flow, ASME 63-HT-34, 1963.

9. Gungor, K.E. and Winterton, R.H.S., A General Correlation for Flow Boiling in Tubes and Annuli, Int. J. Heat Mass Transfer, Vol. 29, pp. 351-358, 1986.

10. Smith, R.A, Boiling Inside Tubes: General Aspects and Saturated Wet-Wall Heat Transfer, ESDU Report 85041, 1985.

11. Levy, S., Forced Convection Subcooled Boiling-Prediction of Vapour Volumetric Fraction, GEAP-5157, 1966.

12. Groeneveld, D.C., Cheng, S.C. and Doan, T., 1986 AECL-UO Critical Heat Flux Look-up Table, Heat Transfer Engineering, Vol. 7, No. 1-2, pp. 46-62, 1986.

13. CHF Predictions in Vertical Tubes, Data Item, ESDU Report 86032, 1986.

14. Groeneveld, D.C., A General CHF Prediction Method for Water, Suitable for Reactor Accident Analysis, C.E.N.G. Report DRE/STT/SETRE/82-2-E/DG, 1982.

15. Taitel, Y. and Dukler, A.E., A Model for Predicting Flow Regime Transitions in Horizontal and Near Horizontal Gas-Liquid Flow, ASME 75-WA/HT-29, 1975, and also AIChE J. Vol. 22, pp. 47-55, 1976.

16. Taitel, Y. and Dukler, A.E., Flow Pattern Transition in Gas-Liquid Systems: Measurement and Modelling, Multiphase Science and Technology, Vol. 11, pp. 1-94, 1986.

17. Groeneveld, D.C. and Stewart, J.C., The Minimum Film Boiling Temperature for Water During Film Boiling Collapse, 7th Int. Heat Transfer Conf., Munich, FRG, 1982.

18. Groeneveld, D.C. and Delorme, G.G.J., Prediction of Thermal Non-Equilibrium in the Post-Dryout Regime, Nuc. Eng. Des., Vol. 36, pp. 17-26, 1976.

19. Berenson, D.J., Film Boiling Heat Transfer from a Horizontal Surface, ASME, J. of Heat Transfer, pp. 351-358, 1961.

20. Laperrier, A., An Analytical and Experimental Investigation of Forced Convective Film Boiling, M.A.Sc. Thesis, University of Ottawa, 1983.

21. Hadaller, G. and Banerjee, S., Heat Transfer to Superheated Steam in Round Tubes, Atomic Energy of Canada Limited, Internal Report WDI-147, 1969.

22. Groeneveld, D.C., Kiameh, B.P., and Cheng, S.C., Prediction of Critical Heat Flux (CHF) for Non-Aqueous Fluids in Forced Convective Boiling, Proceedings 8th International Heat Transfer Conf., San Francisco, U.S.A., Vol. 5, pp 2209-2214, August, 1986.

23. Groeneveld, D.C., Leung, L.K.H., Kiameh, B.P., and Cheng, S.C., A Universal Method for Predicting Critical Heat Flux (CHF) for Aqueous and Non-Aqueous Fluids in Forced Convective Boiling, HTFS Research Symposium, Edinburgh, U.K., September, 1986.

24. Katto, Y. and Ohno, H., An Improved Version of the Generalized Correlation of Critical Heat Flux for the Forced Convective Boiling in Uniformly Heated Vertical Tubes, Int. J. Heat Mass Transfer, Vol. 27, pp. 1641-1648, 1983.

25. Tong, L.S. and Weisman, J., Thermal Analysis of Pressurized Water Reactor, American Nuclear Society, 1970.

26. MATPRO- Version 11, A Handbook of Material Properties for Use in the Analysis of Light Water Reactor Fuel Rod Behaviours, TREE-NUREG-1005, 1981.

27. IBM Professional Fortran Computer Reference Manual, 1984.

28. Jeffreys, H., On The Formation of Water Waves by Wind, I and II, Proc. R. Soc. London A107:189-206, 1925.

29. Jeffreys, h., On The Formation of Water Waves by Wind, Proc.R. Soc. London A110: 241, 1926.

30. Irvine, T.F., Jr. and Liley, P.E., Steam and Gas Tables with Computer Equations, Academic Press Inc., Orlando, Florida, 1984.

31. Meyer, C.A., et al., 1967 ASME Steam Tables, 2nd Edition, ASME, New York, 1967.

32. Schmidt, E., VDI-Steam Tables, 7th Edition, Springer Verlag, Munich, 1968.

Table 1. Critical Heat Flux Look-Up Table ($kW.m^{-2}$) [12]

PRESS	G	QUALITY																			
(KPA)	(KG/M.M.S)	-0.50	-0.40	-0.30	-0.20	-0.15	-0.10	-0.05	0.00	0.05	0.10	0.15	0.20	0.25	0.30	0.40	0.50	0.60	0.70	0.80	0.90	1.00
100	0					3930	3430	2045	1200	1000	900	800	790	780	710	480	470	454	339	225	84	
100	50					4008	3500	2400	1700	1600	1500	1300	1250	1204	1120	899	850	800	501	355	150	
100	100					4800	4200	3100	2200	2100	2000	1450	1000	1000	951	950	950	900	660	430	235	
100	200					5600	4900	3800	2600	2550	2500	1500	1400	1300	1246	1200	1224	1100	854	474	460	
100	300					6400	5600	4500	3000	3000	3000	2500	2400	2300	2300	2166	1721	1448	818	48.	450	
100	500					7200	6300	5200	3600	3550	3500	3200	3000	2500	2358	2350	2301	1220	700	651	440	
100	750					8000	7000	5900	5500	5000	4700	4249	4006	3104	3081	2933	2407	1317	911	700	400	
100	1000					8800	7600	6600	4800	4600	4404	3800	3600	3300	3300	3250	2503	1552	1100	600	300	
100	1500					9600	8200	7000	5500	4800	4600	4500	4451	4280	4000	3911	3105	2601	1100	600	300	
100	2000					10000	8800	7700	6000	5400	5300	5200	5100	5050	5000	4900	4549	2900	1100	600	300	
100	3000					10500	9400	8400	6500	6300	6000	5800	5700	5400	5300	5200	3900	2700	1100	600	300	
100	4000					11000	10000	9000	6900	6785	6650	6100	5300	5000	4600	4000	3000	2000	1000	500	300	
100	5000					11500	10600	9500	8000	7875	7600	7400	5200	4400	3800	3000	2500	1500	900	500	300	
100	7500					12000	11500	11000	10500	9233	9000	7500	5000	4000	3000	2200	2000	1200	800	400	300	
150	0				6273	4000	3500	2400	1350	1200	1100	1000	950	930	913	588	550	544	375	250	116	
150	50				6344	4100	3600	2700	1900	1800	1700	1500	1450	1416	1329	1002	900	873	539	419	400	
150	100				6397	4800	4200	3200	2400	2200	2000	1900	1800	1400	1093	1000	950	941	701	450		
150	200				6488	5400	4800	3500	2700	2600	2500	2100	1600	1400	1200	1200	1166	1150	1100	1000	500	
150	300				6571	6000	5400	4000	3000	2900	2800	2500	2400	1500	1400	1340	1300	1200	1200	800	500	
150	500				6721	6600	6000	4500	3700	3600	3500	3100	2700	1600	1500	1500	1400	1200	1100	670	450	
150	750				7400	7200	6600	5000	4300	4150	4000	3500	2800	1400	1399	1300	1200	1100	1000	650	400	
150	1000				8000	7800	7200	5500	5200	4500	3985	3400	3200	1200	1105	1100	1100	1000	1000	600	350	
150	1500				8600	8400	7600	6000	5500	4000	3800	3300	3100	2400	2000	1500	1300	1200	1100	550	300	
150	2000				9200	9000	8200	6200	5700	4700	4300	4100	4000	3500	3000	2500	2000	1700	1500	550	300	
150	3000				9800	9600	8240	5800	4800	4400	4300	4200	4100	3800	3300	3250	3200	2500	1000	500	300	
150	4000				10200	10000	6636	6000	5000	4600	4500	4300	4200	3600	2800	2800	2600	2000	1000	450	300	
150	5000				10700	10500	9900	9200	9145	7405	6500	5700	4000	3100	2600	2300	2000	1500	900	450	300	
150	7500				11200	11000	10400	9700	9500	8881	8000	6500	5000	3000	2200	1800	1600	1000	600	400	300	
200	0				5971	4820	3700	2774	1450	277	262	248	233	219	204	175	146	117	87	58	29	
200	50				6044	4955	4000	3094	2313	1794	1641	1562	1483	1405	1326	1244	1044	650	600	574	571	
200	100				6099	5000	4100	3200	2600	2300	2100	2000	1900	1300	1200	1109	800	767	750	750	516	
200	200				6193	5200	4300	3400	2800	2500	2300	2150	1400	1297	1200	1180	1100	1000	1000	1000	514	
200	300				6278	5400	4450	3580	3000	2700	2400	2200	2150	2100	2000	1829	1497	904	617	400	350	
200	500				6433	5600	4650	3700	3150	2900	2500	2400	2300	2250	2226	1759	1388	659	250	200	200	
200	750				6610	5800	4850	3900	3300	3000	2650	2500	2314	2159	1818	1590	1463	1000	600	450	300	
200	1000				6775	6000	5000	4000	3400	3000	2600	2500	2134	1939	1800	1700	1600	1000	600	450	300	
200	1500				7083	6200	4600	3800	3300	3000	2600	2500	2350	2169	1800	1700	1500	1000	600	450	300	
200	2000				7370	6400	4500	4000	3500	3000	2600	2500	2150	2050	1800	1700	1400	1000	600	450	300	
200	3000				7905	7000	5742	4287	3900	3000	2600	2500	2150	2050	1800	1700	1400	1000	600	450	300	
200	4000				8600	8500	6411	4800	4500	3000	2600	2500	2150	2050	1800	1700	1400	1000	600	450	300	
200	5000				8880	6607	6120	5267	4845	3000	2600	2500	2150	2050	1800	1700	1400	1000	600	450	300	
200	7500				9990	6990	6465	5581	5077	3000	2600	2500	2150	2050	1800	1700	1400	1000	600	450	300	
300	0				5631	4650	3667	2683	1700	325	308	291	274	257	240	205	171	137	103	68	34	
300	50				5712	5063	4292	3296	2975	2481	2327	2248	2168	2014	1860	1551	1067	535	500	500	450	
300	100				5772	5200	4500	3500	3400	3200	3000	2900	2800	2600	2400	1160	900	870	850	800	504	
300	200				5877	5600	4700	3600	3500	3200	2900	2800	1600	1463	1400	1400	1376	1300	1200	1181	569	
300	300				5971	4592	3324	3300	3250	3200	2800	2700	2600	2500	2400	2176	1785	1043	438	400	362	
300	500				6142	4634	3367	3300	3250	3200	2700	2600	2600	2600	2500	1946	1341	811	200	200	200	
300	750				6338	6000	5000	3900	3800	3200	2800	2700	2586	2475	2402	1526	868	490	418	250	200	
300	1000				6521	6200	5200	4000	3900	3200	2600	2500	2395	2208	2100	1800	1500	1200	700	400	200	
300	1500				6862	6400	4154	4100	4000	3200	2600	2600	2538	2360	2100	1800	1500	1200	700	400	200	
300	2000				7180	6600	4300	4200	4100	3200	2600	2500	2294	2200	2100	1800	1500	1200	700	400	200	
300	3000				8000	7778	5690	4800	4706	3200	2600	2500	2294	2200	2100	1800	1500	1200	700	400	200	
300	4000				8600	8443	6302	4518	4400	3200	2600	2500	2294	2200	2100	1800	1500	1200	700	400	200	
300	5000				8852	5419	4851	3967	3525	3200	2600	2500	2294	2200	2100	1800	1500	1200	700	400	200	
300	7500				10082	5816	5198	4236	3630	3200	2600	2500	2300	2200	2100	1800	1500	1200	700	400	200	
450	0				5363	4540	4222	2000	1968	380	360	340	320	300	280	240	200	160	150	120	110	
450	50				5454	5035	4627	2330	2250	2195	2115	2035	1993	1950	1870	1860	1625	600	550	543	500	
450	100				5522	5200	4100	3400	2900	2800	2700	2600	2550	2200	2000	1500	1123	1112	984	908	595	
450	200				5639	5600	4150	3400	3000	2800	2600	2550	2500	2200	1700	1600	1500	1400	1306	890	595	
450	300				5745	4145	2896	2850	2825	2800	2600	2500	2450	2400	2400	2300	2161	1583	755	447	408	
450	500				5939	4187	2939	2900	2850	2800	2600	2400	2400	2400	2300	2245	1784	1123	451	250	236	
450	750				6159	6000	4300	3400	3100	2800	2600	2300	2150	2000	1900	1355	879	707	467	350	316	
450	1000				6365	6200	4400	3400	3200	2800	2600	2100	1966	1786	1200	700	606	593	500	300	200	
450	1500				6749	6400	4145	3060	3000	2800	2600	2100	2086	1500	1000	700	665	600	500	300	200	
450	2000				7108	6600	3521	3400	3300	2800	2600	2100	1800	1500	1200	1100	1000	700	500	300	200	
450	3000				7775	7500	5752	4146	3716	2800	2600	2200	1800	1500	1200	1100	1000	700	500	300	200	
450	4000				8399	8000	6210	4292	4076	2800	2600	2200	1800	1500	1200	1100	1000	700	500	300	200	
450	5000				8991	6619	6002	5440	3500	2800	2600	2200	1900	1500	1200	1100	1000	700	500	300	200	
450	7500				10376	6878	6271	5707	3600	2800	2600	2200	2000	1500	1200	1100	1000	700	500	300	200	
700	0			6548	5153	4482	4264	2059	1488	448	424	401	377	354	330	283	236	189	97	72	70	
700	50			6652	5260	5021	4669	2488	2300	2212	2056	1825	1594	1363	1133	971	809	500	450	404	400	
700	100			6730	5339	5200	4200	3500	3000	2800	2600	2300	2000	1700	1400	1200	1000	830	820	816	578	
700	200			6865	5477	5300	4250	3600	3200	3000	2900	2700	2600	2500	2200	2000	1800	1700	1403	913	649	
700	300			6986	5601	5400	4300	3700	3400	3000	2900	2700	2600	2550	2500	2500	2500	1892	1093	628	533	
700	500			7208	5827	5700	4400	3800	3500	3000	2900	2800	2700	2650	2600	2600	2568	1360	644	385	353	
700	750			7460	6085	6000	4600	3900	3600	3000	2700	2600	2500	2400	2300	2284	1398	680	450	426	420	
700	1000			7696	6326	6200	5060	4094	3600	3000	2800	2700	2700	2695	1600	1595	914	467	260	250	200	
700	1500			8136	6775	6400	4991	4025	3600	3000	2500	2400	2300	2284	1200	1166	745	259	199	175	150	
700	2000			8547	7195	6600	5200	4400	3600	3000	2500	2200	1800	1500	1300	1300	900	250	200	200	150	
700	3000			9312	7976	6800	5400	4600	3600	3000	2500	2200	1800	1500	1300	1200	900	250	200	200	150	
700	4000			10020	8705	7000	5600	4800	3600	3000	2500	2200	1800	1500	1300	1200	900	250	200	200	150	
700	5000			10705	9397	7200	5800	4900	3600	3000	2500	2200	1900	1500	1300	1200	900	250	200	200	150	
700	7500			12294	11018	7400	6000	5000	3600	3000	2500	2200	2000	1600	1300	1200	900	250	200	200	150	
1000	0			8092	6551	4480	3864	3240	2620	509	483	456	429	402	375	322	268	214	161	107	54	
1000	50			8195	6657	5670	5092	4560	4105	3427	3271	3114	3032	2801	2569	2330	1942	1104	875	814	424	
1000	100			8271	6736	6000	5500	5000	4600	4400	4200	4000	3900	3600	3300	3000	2500	1600	1547	1070	654	
1000	200			8403	8100	8000	7500	7000	6000	5800	5600	5400	5100	4700	4400	4300	3352	2455	1704	1117	778	
1000	300			8522	8200	8000	7500	7000	6500	6300	5600	5400	5100	4700	4700	4671	3958	2571	1569	918	711	
1000	500			8738	8306	8000	7500	7000	6500	6200	5600	5400	5100	4700	4652	4600	3803	2087	1123	603	437	
1000	750			8985	8400	8000	7500	7000	6500	6100	5600	5400	5000	4900	4800	3940	2272	1106	696	527	466	
1000	1000			9217	8500	8000	7500	7000	6500	6000	5600	5400	5109	4923	4123	2905	1646	888	606	298	218	
1000	1500			9647	8500	8000	7500	7000	6500	5900	5300	5000	4925	4425	3325	2393	1328	613	256	188	100	
1000	2000			10049	8700	8000	7500	7000	6500	5700	5200	4800	4400	3600	3500	3474	2807	800	250	150	100	
1000	3000			10798	9362	8000	7500	7000	6500	5500	5100	4700	4200	4000	3962	3858	1300	750	250	150	100	
1000	4000			11497	10088	8000	7500	7000	6500	5300	5000	4500	4000	3400	2800	1850	1150	700	250	150	100	
1000	5000			12161	10778	8000	7500	7000	6500	5400	4900	4400	3800	3300	2600	1650	1000	650	250	150	100	
1000	7500			13796	12391	8000	7500	7000	6500	5000	4800	4300	3600	3200	2300	1500	900	600	250	150	100	

Table 1. (cont'd)

PRESS (KPA)	G (KG/M.M.S)	0.50	0.40	0.30	0.20	0.15	0.10	0.05	QUALITY 0.00	0.05	0.10	0.15	0.20	0.25	0.30	0.40	0.50	0.60	0.70	0.80	0.90	1.00
100	0					1930	1430	2040	2200	1000	980	800	790	780	10	480	470	450	330	225	89	
100	50					4000	1500	2400	1700	1600	1500	1300	1250	1204	1120	895	850	800	501	355	350	
100	100					3100	4200	3100	2200	2100	2000	1450	1000	1000	955	950	950	900	660	430	335	
100	200					4600	4900	4800	2600	2550	2500	1500	1400	1300	1246	1200	1174	1100	854	474	460	
100	300					6400	5600	4500	3000	3000	3000	2500	2400	2300	2300	2166	1721	1448	818	481	450	
100	500					7200	6300	5200	3600	3550	3500	3200	3000	2500	2358	2350	2301	1220	700	651	440	
100	750					8000	7000	5900	5500	5000	4700	4249	4006	3104	3081	2933	2407	1317	911	700	400	
100	1000					8800	7600	6600	4800	4600	4406	3800	3600	3300	3300	3250	2503	1552	1100	600	300	
100	1500					9600	8200	7000	5500	4800	4600	4500	4451	4200	4000	3911	3105	2601	1100	600	300	
100	2000					10000	9800	7700	6000	5400	5300	5200	5100	5050	5000	4900	4549	2900	1100	600	300	
100	3000					10500	9400	8400	6500	6300	6000	5800	5700	5400	5300	5200	3900	2700	1100	600	300	
100	4000					11000	10000	9000	6900	6785	6650	6100	5300	5000	4600	4000	3000	2000	1000	500	300	
100	5000					11500	10600	9500	8000	7875	7600	7400	5200	4400	3800	3000	2500	1500	900	500	300	
100	7500					12000	11500	11000	10500	9233	9000	7500	5000	4000	3000	2200	2000	1200	800	400	300	
150	0				6275	4000	3500	2400	1350	1200	1100	1000	950	930	913	588	550	544	375	250	116	
150	50				6344	4100	3600	2700	1900	1800	1700	1500	1450	1416	1329	1002	900	873	539	419	400	
150	100				6397	4800	4200	3200	2400	2200	2000	1900	1800	1400	1093	1000	950	950	941	701	450	
150	200				6488	5400	4800	3500	2700	2600	2500	2100	1600	1400	1200	1200	1166	1150	1100	1000	500	
150	300				6571	6000	5400	4000	3000	2900	2800	2500	2400	1500	1400	1340	1300	1200	1200	800	500	
150	500				6721	6600	6000	4500	3700	3600	3500	3100	2700	1600	1500	1500	1400	1200	1100	670	450	
150	750				7400	7200	6600	5000	4300	4150	4000	3500	2800	1400	1399	1300	1200	1100	1000	650	400	
150	1000				8000	7800	7200	5500	5200	4500	3985	3400	3200	1200	1105	1100	1100	1000	1000	600	350	
150	1500				8600	8400	7600	6000	5500	4000	3800	3300	3100	2400	2000	1500	1300	1200	1100	550	300	
150	2000				9200	9000	8200	6200	5700	4700	4300	4100	4000	3500	3000	2500	2000	1700	1500	550	300	
150	3000				9800	9600	8240	6240	5800	4800	4400	4300	4200	4100	3800	3300	3250	3200	2500	1000	500	300
150	4000				10200	10000	6636	6000	5000	4600	4500	4300	4200	3600	2800	2800	2600	2000	1000	450	300	
150	5000				10700	10500	9900	9200	9145	7405	6500	5700	4000	3100	2600	2300	2000	1500	900	450	300	
150	7500				11200	11000	10400	9700	9500	8881	8000	6500	5000	3000	2200	1800	1600	1000	600	400	300	
200	0				5971	4820	3780	2774	1450	277	262	248	233	219	204	175	146	117	87	58	29	
200	50				6044	4955	4000	3094	2313	1794	1641	1562	1483	1405	1326	1244	1044	650	600	574	571	
200	100				6099	5000	4100	3200	2600	2300	2100	2000	1900	1300	1200	1109	800	767	750	750	516	
200	200				6193	5200	4300	3400	2800	2500	2300	2150	1400	1297	1200	1180	1100	1000	1000	1000	514	
200	300				6278	5400	4450	3500	3000	2780	2480	2280	2150	2100	2000	1829	1497	904	417	400	350	
200	500				6433	5600	4650	3700	3150	2900	2590	2400	2300	2250	2226	1759	1388	659	250	200	200	
200	750				6610	5800	4850	3900	3300	3000	2650	2500	2314	2159	1818	1590	1463	1000	600	450	300	
200	1000				6775	6000	5000	4000	3400	3000	2600	2500	2134	1939	1800	1700	1600	1000	600	450	300	
200	1500				7083	6200	4600	3800	3300	3000	2600	2500	2350	2169	1800	1700	1500	1000	600	450	300	
200	2000				7370	6400	4500	4000	3500	3000	2600	2500	2150	2050	1800	1700	1400	1000	600	450	300	
200	3000				7905	7000	5742	4287	3900	3000	2600	2500	2150	2050	1800	1700	1400	1000	600	450	300	
200	4000				8600	8500	6411	4800	4500	3000	2600	2500	2150	2050	1800	1700	1400	1000	600	450	300	
200	5000				8880	6607	6120	5267	4845	3000	2600	2500	2150	2050	1800	1700	1400	1000	600	450	300	
200	7500				9990	6990	6465	5581	5077	3000	2600	2500	2150	2050	1800	1700	1400	1000	600	450	300	
300	0				5631	4650	3667	2683	1700	325	308	291	274	257	240	205	171	137	103	68	34	
300	50				5712	5063	4292	3296	2975	2481	2327	2248	2168	2014	1860	1551	1067	535	500	500	450	
300	100				5772	5200	4500	3500	3400	3200	3000	2900	2800	2600	2400	1160	900	870	850	800	504	
300	200				5877	5600	4700	3600	3500	3200	2900	2800	1600	1463	1400	1400	1376	1300	1200	1181	569	
300	300				5971	4592	3324	3300	3250	3200	2800	2700	2600	2500	2400	2176	1785	1043	438	400	362	
300	500				6142	4634	3367	3300	3250	3200	2700	2600	2600	2600	2500	1946	1341	811	200	200	200	
300	750				6338	6000	5000	3900	3800	3200	2800	2700	2586	2475	2402	1526	868	690	418	250	200	
300	1000				6521	6200	5200	4000	3900	3200	2600	2500	2395	2308	2100	1800	1500	1200	700	400	200	
300	1500				6862	6400	6154	4100	4000	3200	2600	2600	2538	2360	2100	1800	1500	1200	700	400	200	
300	2000				7180	6600	4300	4200	4100	3200	2600	2500	2294	2200	2100	1800	1500	1200	700	400	200	
300	3000				8000	7778	5690	4800	4706	3200	2600	2500	2294	2200	2100	1800	1500	1200	700	400	200	
300	4000				8600	8443	6302	4518	4400	3200	2600	2500	2294	2200	2100	1800	1500	1200	700	400	200	
300	5000				8852	5419	4851	3967	3525	3200	2600	2500	2294	2200	2100	1800	1500	1200	700	400	200	
300	7500				10082	5816	5198	4236	3630	3200	2600	2500	2300	2200	2100	1800	1500	1200	700	400	200	
450	0				5363	4540	4222	2000	1968	380	360	340	320	300	280	240	200	160	150	120	110	
450	50				5454	5035	4627	2330	2250	2195	2115	2035	1993	1950	1870	1860	1625	600	550	543	500	
450	100				5522	5200	4100	3400	2900	2800	2700	2600	2550	2200	2000	1500	1123	1112	984	908	595	
450	200				5639	5600	4150	3400	3000	2800	2600	2550	2500	2200	1700	1600	1500	1400	1306	890	595	
450	300				5745	4145	2896	2850	2825	2800	2600	2500	2450	2400	2400	2300	2161	1583	755	447	408	
450	500				5939	4187	2939	2900	2850	2800	2600	2400	2400	2400	2300	2245	1784	1123	451	250	236	
450	750				6159	6000	4300	3400	3100	2800	2600	2300	2150	2000	1900	1355	879	707	467	350	316	
450	1000				6365	6200	4400	3400	3200	2800	2600	2100	1966	1786	1200	700	606	593	500	300	200	
450	1500				6749	6400	4145	3060	3000	2800	2600	2100	2086	1500	1000	700	665	600	500	300	200	
450	2000				7108	6600	3521	3400	3300	2800	2600	2100	1800	1500	1200	1100	1000	700	500	300	200	
450	3000				7775	7500	5752	4146	3716	2800	2600	2200	1800	1500	1200	1100	1000	700	500	300	200	
450	4000				8399	8000	6210	4292	4076	2800	2600	2200	1800	1500	1200	1100	1000	700	500	300	200	
450	5000				8991	6619	6002	5448	3500	2800	2600	2200	1900	1500	1200	1100	1000	700	500	300	200	
450	7500				10376	6878	6271	5707	3690	2800	2600	2200	2000	1500	1200	1100	1000	700	500	300	200	
700	0			6548	5153	4482	4264	2059	1488	448	424	401	377	354	330	283	236	189	97	72	70	
700	50			6652	5260	5021	4669	2488	2300	2212	2056	1825	1594	1363	1133	971	809	500	450	404	400	
700	100			6730	5339	5200	4200	3500	3000	2800	2600	2300	2000	1700	1400	1200	1000	830	820	816	578	
700	200			6865	5477	5300	4250	3600	3200	3000	2900	2700	2600	2500	2200	2000	1800	1700	1403	913	649	
700	300			6986	5601	5400	4300	3700	3400	3000	2900	2700	2600	2550	2500	2500	2500	1892	1093	628	533	
700	500			7208	5827	5700	4400	3800	3500	3000	2900	2800	2700	2650	2600	2600	2568	1360	644	385	353	
700	750			7460	6085	6000	4600	3900	3600	3000	2700	2600	2500	2400	2300	2284	1398	680	450	426	420	
700	1000			7696	6326	6200	5060	4094	3600	3000	2800	2700	2700	2695	1600	1595	914	467	260	250	200	
700	1500			8136	6775	6400	4991	4025	3600	3000	2500	2400	2300	2284	1200	1166	745	259	199	175	150	
700	2000			8547	7195	6600	5200	4400	3600	3000	2500	2200	1800	1500	1300	1300	900	250	200	200	150	
700	3000			9312	7976	6800	5400	4600	3600	3000	2500	2200	1800	1500	1300	1200	900	250	200	200	150	
700	4000			10026	8705	7000	5600	4800	3600	3000	2500	2200	1800	1500	1300	1200	900	250	200	200	150	
700	5000			10705	9397	7200	5800	4900	3600	3000	2500	2200	1900	1500	1300	1200	900	250	200	200	150	
700	7500			12294	11018	7400	6000	5000	3600	3000	2500	2200	2000	1600	1300	1200	900	250	200	200	150	
1000	0			8092	6551	4480	3866	3240	2620	509	483	456	429	402	375	322	268	214	161	107	54	
1000	50			8195	6657	5020	3893	4560	4105	3427	3271	3114	3032	2801	2569	2330	1942	1104	875	814	626	
1000	100			8271	6736	6000	5500	5000	4600	4400	4200	4000	3900	3600	3300	3000	2500	1600	1547	1070	659	
1000	200			8403	8100	8000	7500	7000	6800	5800	5600	5400	5100	4700	4400	4300	3352	2455	1704	1117	778	
1000	300			8522	8200	8000	7500	7000	6500	6300	5600	5400	5100	4700	4700	4671	3958	2571	1569	918	711	
1000	500			8738	8300	8000	7500	7000	6500	6200	5600	5400	5100	4700	4652	4600	3803	2087	1123	603	437	
1000	750			8985	8400	8000	7500	7000	6500	6100	5600	5400	5000	4900	4800	3940	2272	1106	696	527	466	
1000	1000			9217	8500	8000	7500	7000	6500	6000	5600	5400	5369	4923	4123	2905	1646	888	606	298	218	
1000	1500			9647	8500	8000	7500	7000	6500	5900	5300	5000	4925	4425	3325	2393	1328	613	256	188	100	
1000	2000			10049	8700	8000	7500	7000	6500	5700	5200	4800	4400	3600	3500	3474	2807	800	250	150	100	
1000	3000			10798	9362	8000	7500	7000	6500	5500	5100	4700	4200	4000	3962	3858	1300	750	250	150	100	
1000	4000			11497	10008	8000	7500	7000	6500	5300	5000	4500	4000	3400	2800	1850	1150	700	250	150	100	
1000	5000			12161	10778	8000	7500	7000	6500	5400	4900	4400	3800	3300	2600	1650	1000	650	250	150	100	
1000	7500			13716	12391	8000	7500	7000	6500	5500	4800	4300	3600	3200	2300	1500	900	600	250	150	100	

Table 2. CHF Correction Factors [14]

Factor	Form	Comments
K_1, subchannel or tube cross section factor	For 0.002 m < D_h < 0.016 m $K_1 = \left(\frac{0.008}{D_h}\right)^{1/3}$ For D_h > 0.016 m $K_1 = \left(\frac{0.008}{0.016}\right)^{1/3} = 0.79$	Includes the observed diameter effect on CHF This effect is quality-dependent and could be included by replacing the exponent 1/3 by (2 − X)/4 (requires verification)
K_2, bundle factor	$K_2 = \min[0.8, 0.8\exp(-0.5X^{1/3})]$	Predicts the correct trend of quality on the bundle correction factor
K_3, grid spacer factor	$K_3 = 1 + A\exp(-B\,L_{sp}/D_h)$ $A = 1.5K^{0.5}\left(\frac{G}{1000}\right)^{0.2}$, $B = 0.10$	Ideally A and B should be obtained for each grid spacer as the pressure loss coefficient K is insufficient to completely express the grid spacer effect
K_4, heated length factor	$L/D_h \geq 5$: $K_4 = \exp\left(\frac{D_h}{L}e^{2\alpha}\right)$ α evaluated from homogeneous model $\alpha = X/[X + \rho_g/\rho_f(1 - X)]$	Inclusion of α correctly predicts the diminishing length effect at subcooled conditions. The length effect is particularly noticeable if L/D_h < 10 for subcooled burnout and L/D_h < 100 for two-phase dryout
K_5, axial flux distribution factor	$X > 0$: $K_5 = q_{BLA}/q_{LOCAL}$ $X < 0$: $K_5 = 1.0$	Tong's [17] F factor may also be used but only within narrow ranges of conditions
K_6, flow factor, horizontal flow	Stratified flow ($G < G_1$) $K_6 = 0.0$ Nonstratified flow ($G > G_2$) $K_6 = 1.0$ Intermediate ($G_1 < G < G_2$) $K_6 = \frac{G - G_1}{G_2 - G_1}$	G_1 mass flux boundary between fully stratified and intermittent flow (kg/m^2 s) G_2 mass flux boundary between intermittent and annular flow (kg/m^2 s) To find G_1 and G_2 use Taitel and Dukler's [18] flow regime map
K_7, flow factor, vertical flow	$G < -400$ kg/m^2 s or $X = 0.0$ $K_7 = 1.0$ $-50 < G < 10$ kg/m^2 s CHF = CHF$_{G=0,X=0}(1 - \alpha C_1)$ $10 < G < 100$ kg/m^2 s $-400 < G < -50$ kg/m^2 s } linear interpolation	$\alpha < 0.8$ $C_1 = 1.0$ $\alpha > 0.8$ $C_1 = \frac{0.8 + 0.2\rho_g/\rho_f}{\alpha + (1 - \alpha)\rho_g/\rho_f}$

TABLE 3: SUMMARY OF FUNCTION KEYS

<↓>	Cursor go down one input area
<←>	Cursor go to the left input area
<→>	Cursor go to the right input area
<↑>	Cursor go up one input area
<Return>	Cursor go to next input area
<BackSpace>	Erase previous input character
<Ctrl-End>	Input page termination
<Shift-PrtSc>	Print screen material on paper using a printer
<ESC>	Program termination during input stage

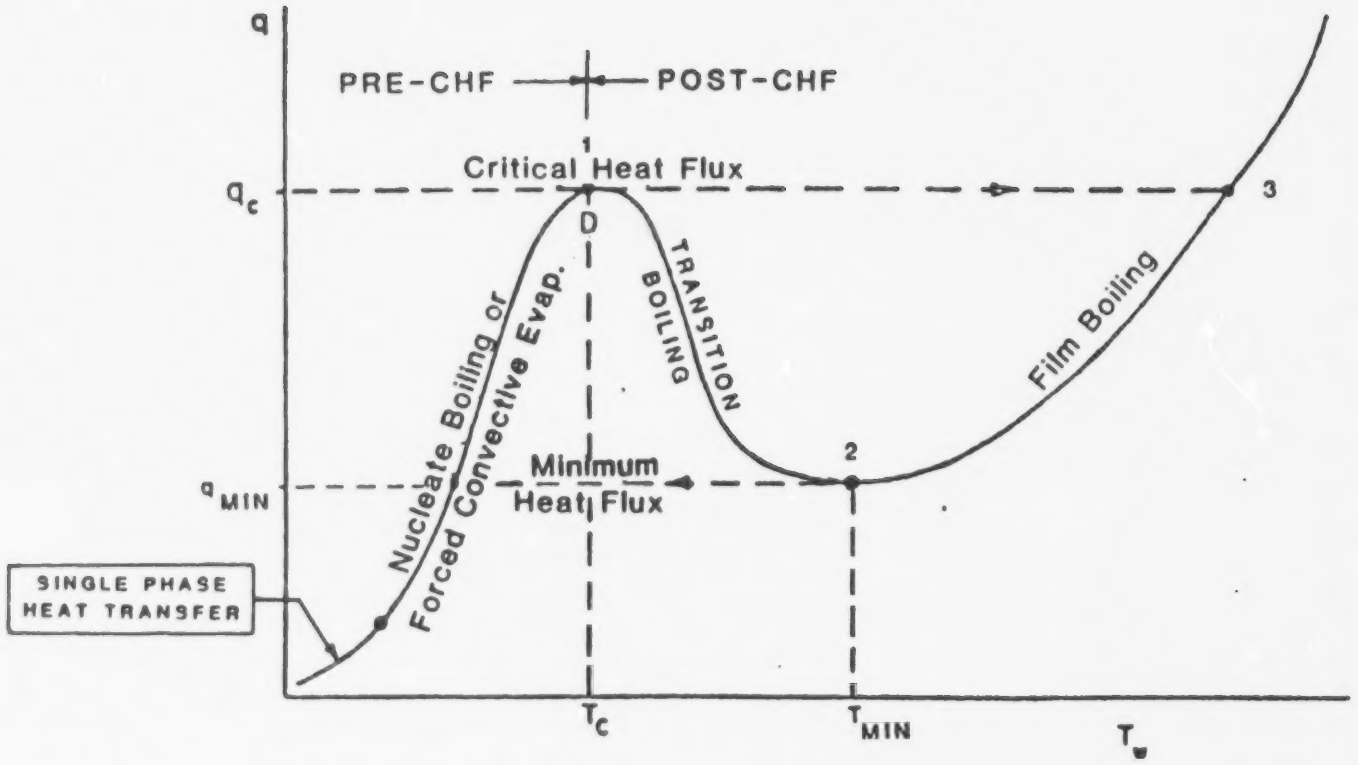

Figure 1. Schematic Diagram of a Boiling Curve

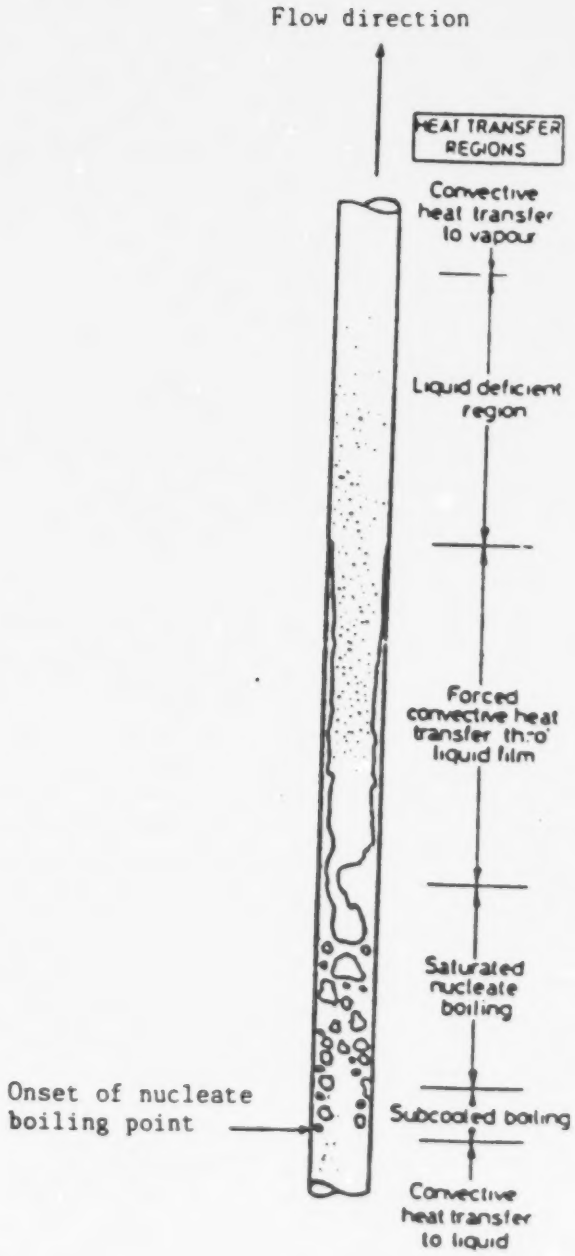

Figure 2. Regions of Heat Transfer in Convective Boiling [1]

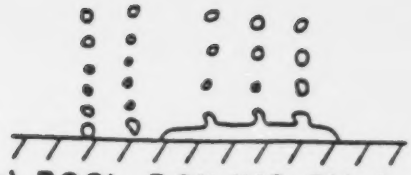

(a) POOL BOILING ON A HORIZONTAL SURFACE

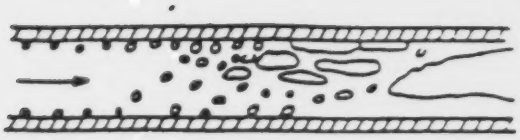

(b) CONVECTIVE BOILING IN HORIZONTAL FLOW

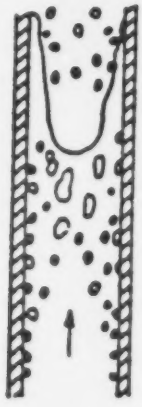

(c) CONVECTIVE BOILING INSIDE VERTICAL TUBES

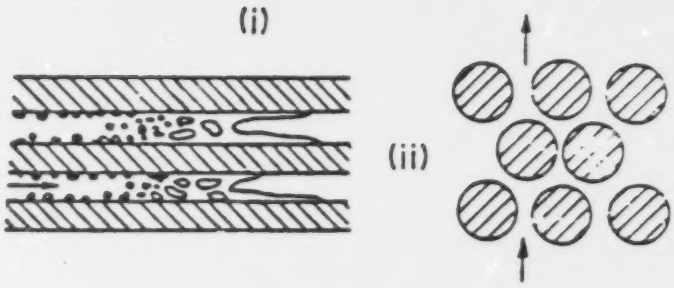

(d) BOILING IN HORIZONTAL BUNDLES
(i) AXIAL FLOW (ii) CROSS FLOW

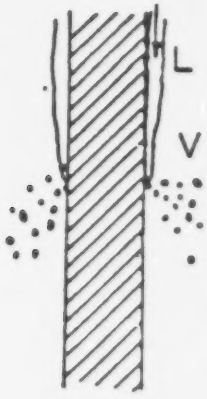

(e) HEAT TRANSFER DURING TOP FLOODING

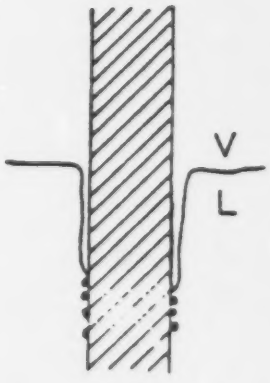

(f) HEAT TRANSFER DURING BOTTOM FLOODING

Figure 3. Heat Transfer Configuration [2]

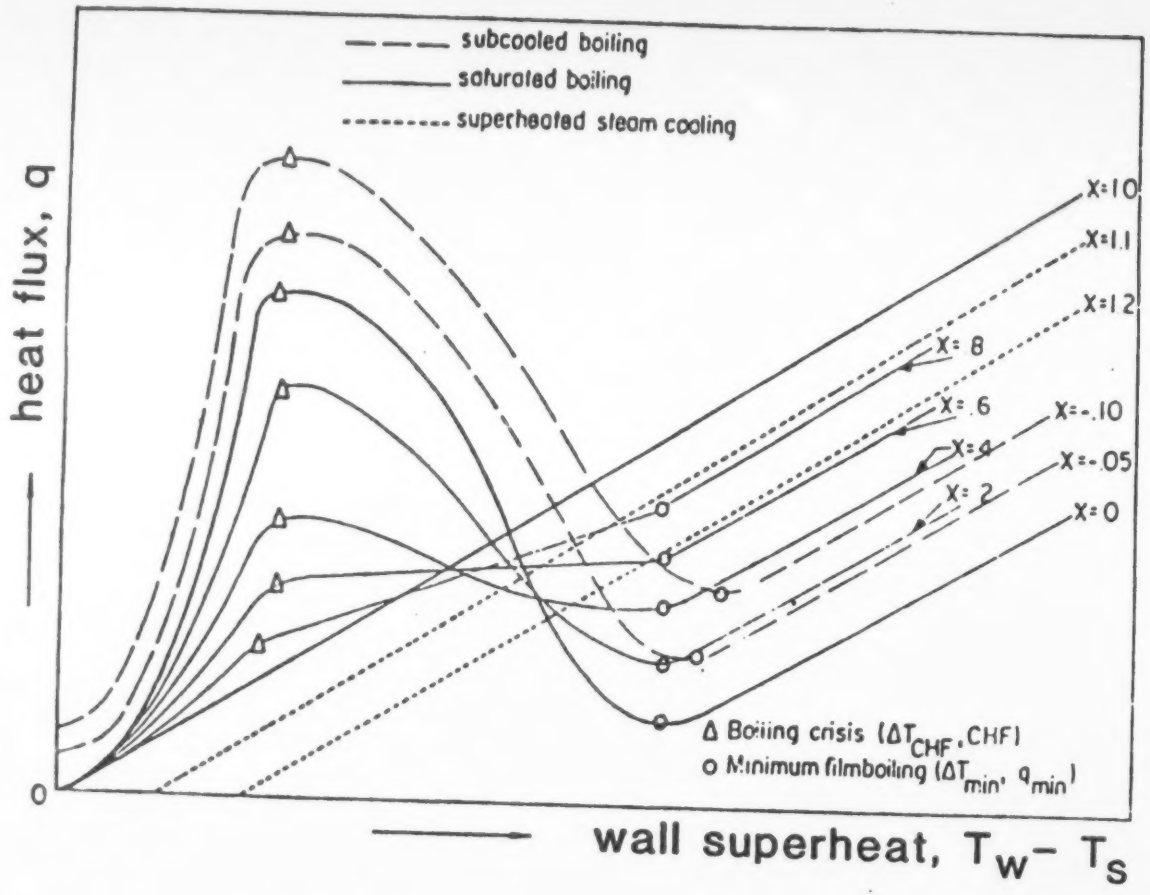

Figure 4. Effect of Quality on Boiling Curve [2A]

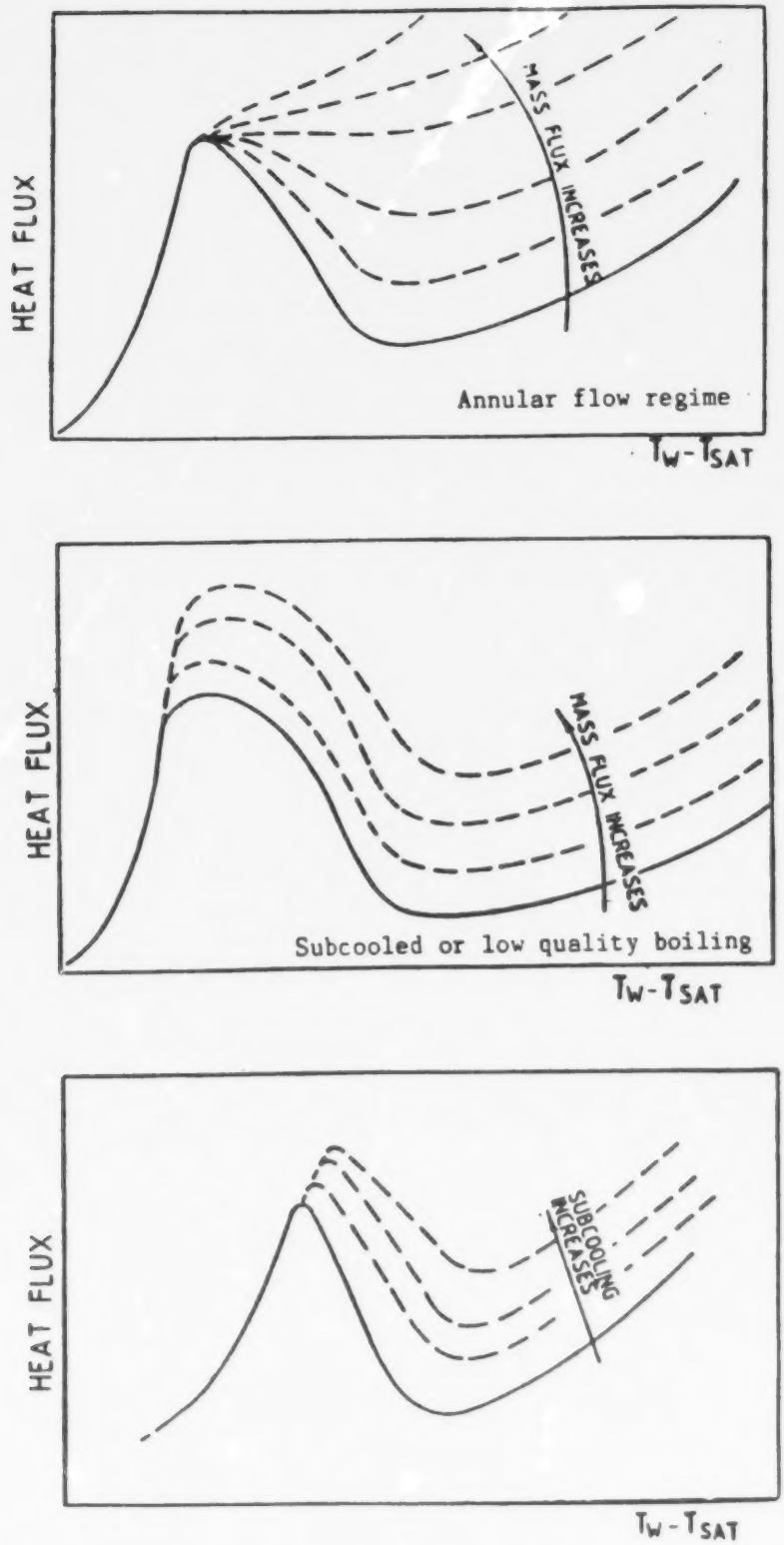

Figure 5. Effect of Mass Flux and Subcooling on Boiling Curve

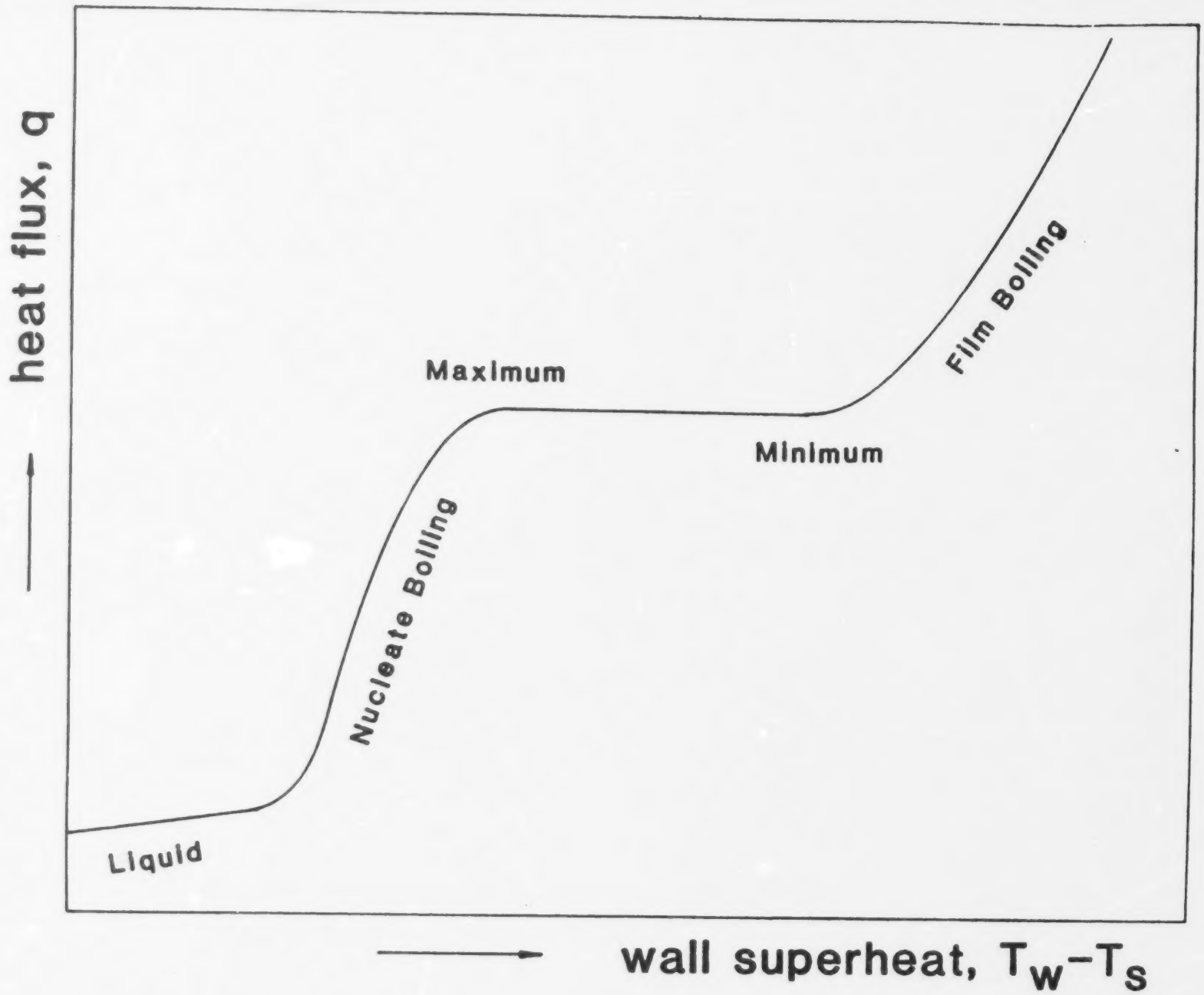

Figure 6. Boiling Curve for a Heat Flux Controlled System

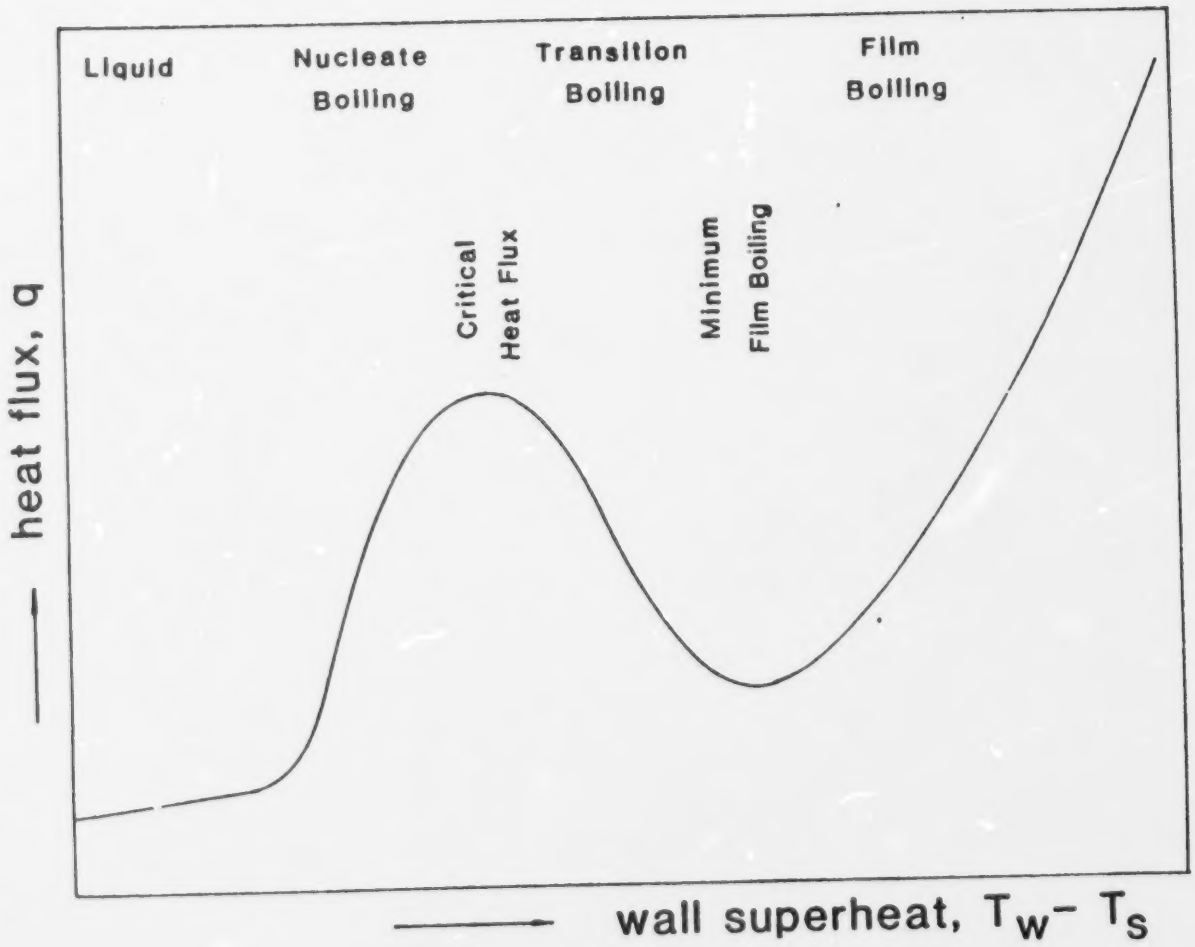

Figure 7. Boiling Curve for a Temperature Controlled System

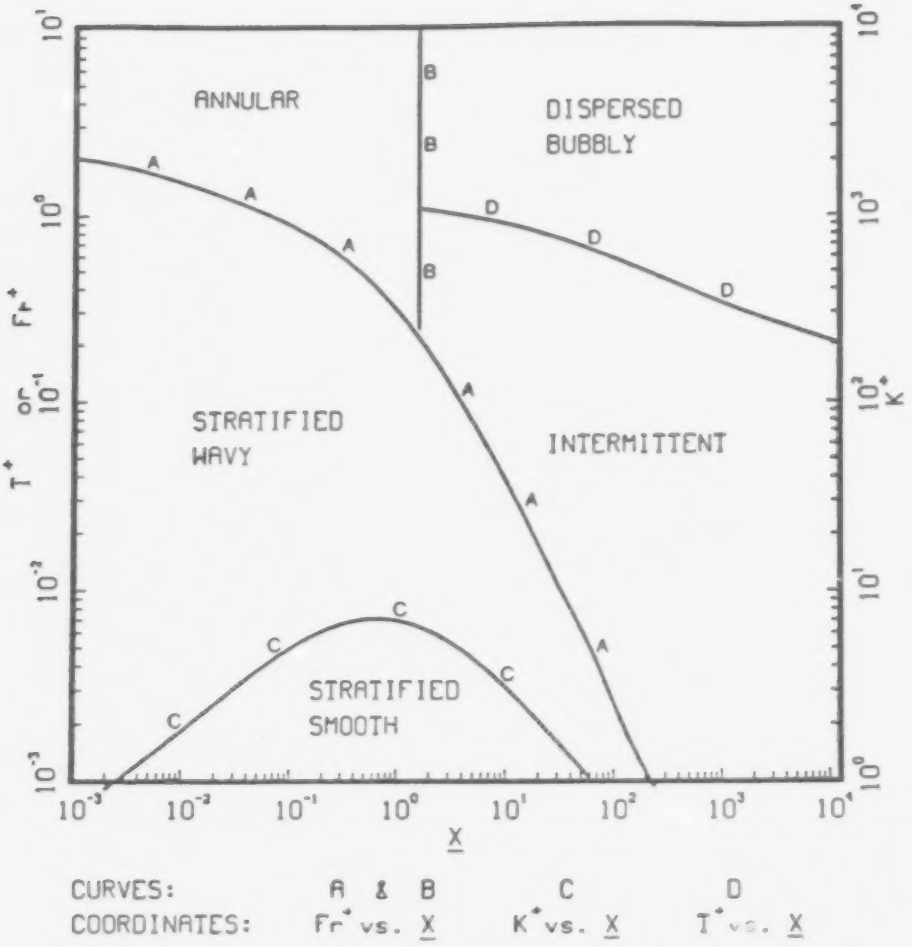

Figure 8. Generalized Flow Regime Map for Horizontal Flow [14]

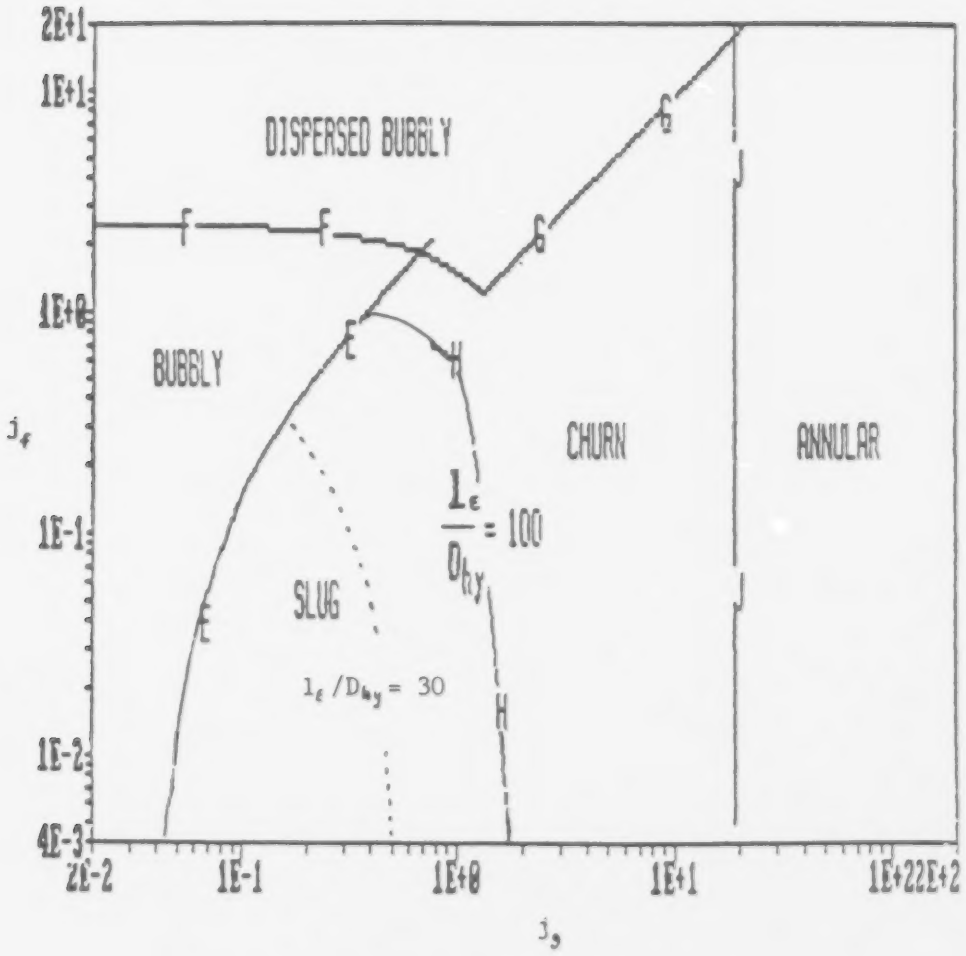

Figure 9. Flow Regime Map for Steam-Water Upward Flow in a 5.1 cm Diameter Tube at 1.0 atm

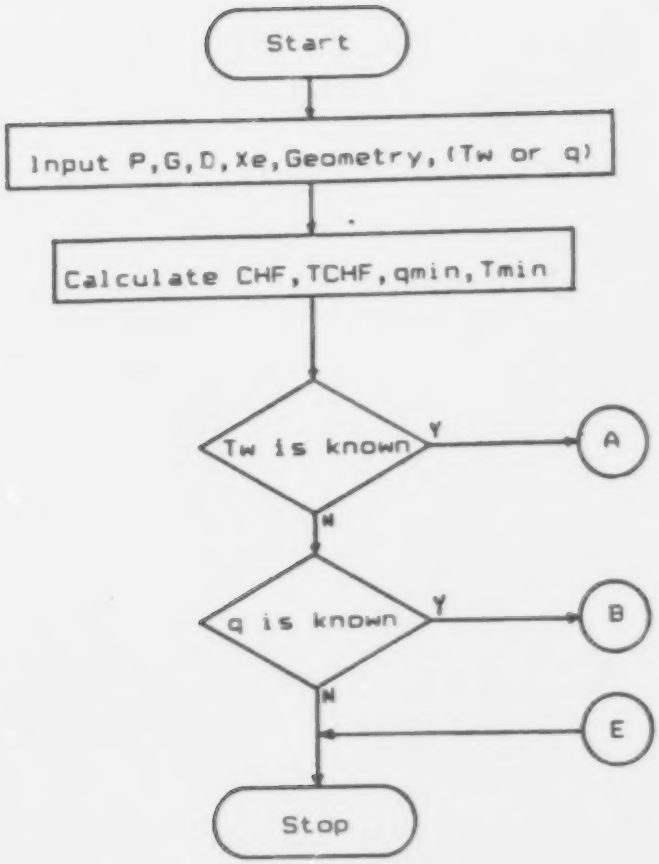

Figure 10. Start-up Stage of the Heat Transfer Logic

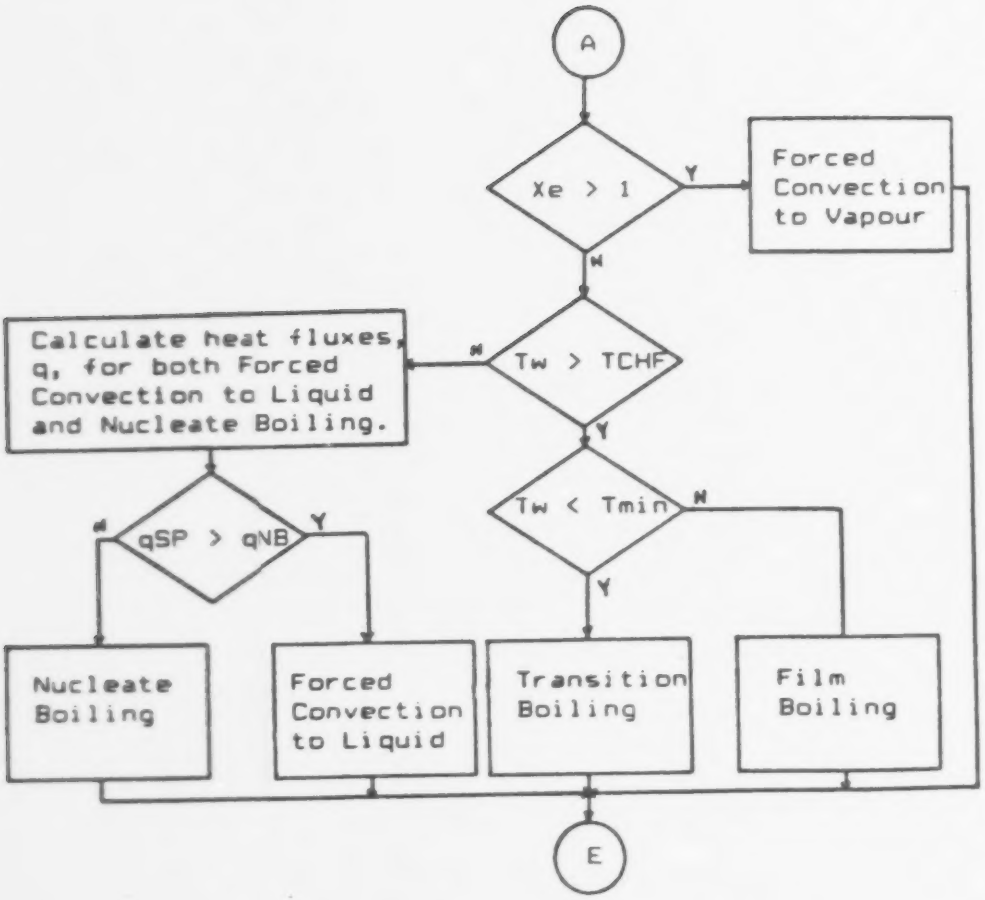

Figure 11. Heat Transfer Logic for a Temperature Controlled Mode

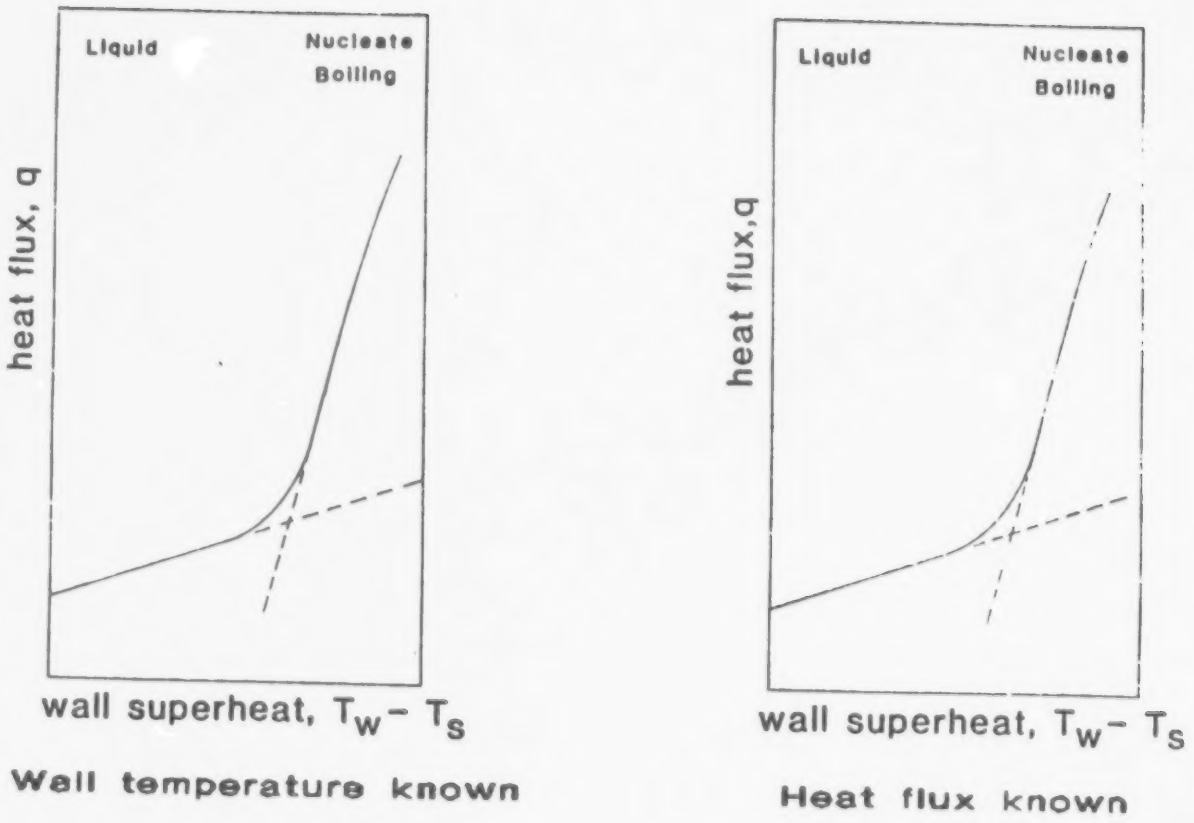

Figure 12. Transition from Single-Phase Forced Convection to Nucleate Boiling

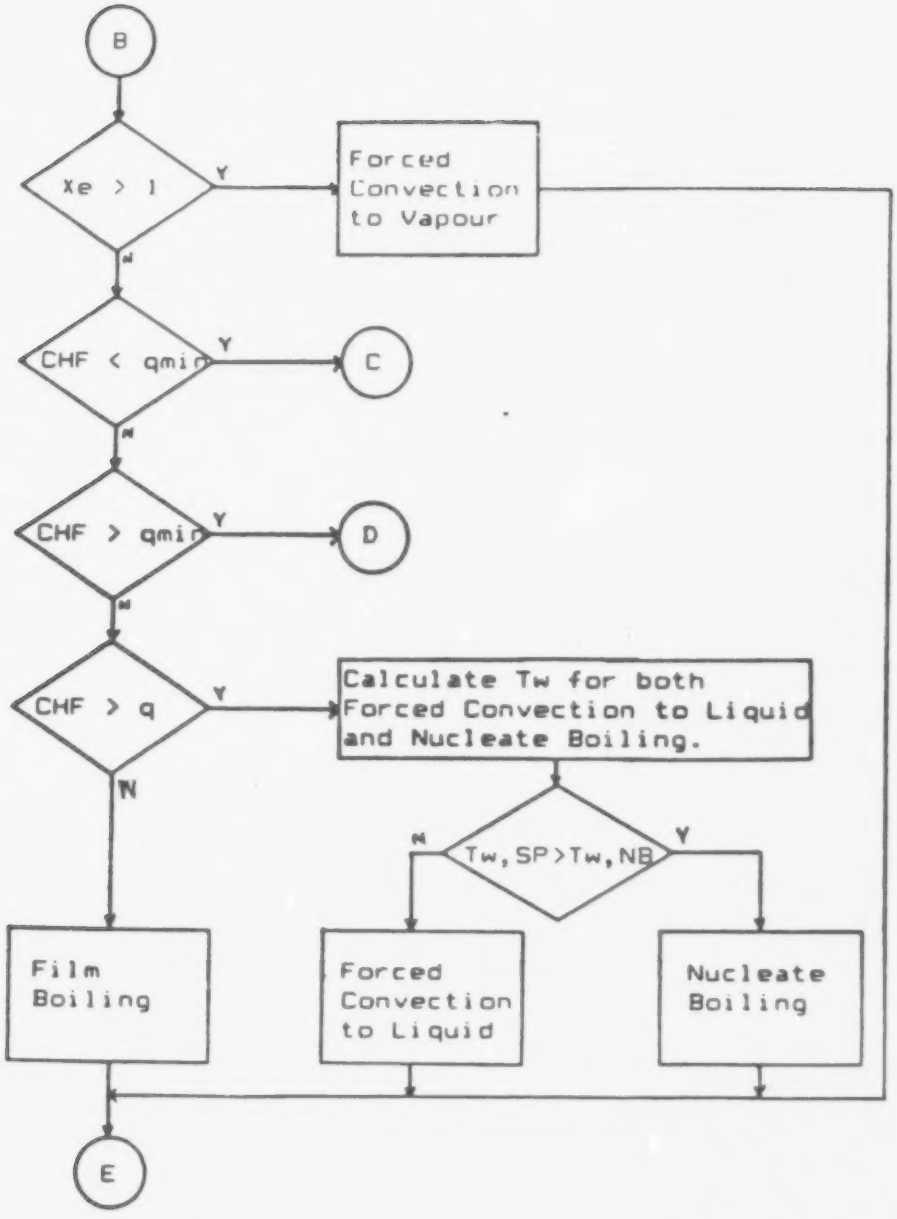

Figure 13. Heat Transfer Logic for a Heat Flux Controlled Mode (CHF = qmin)

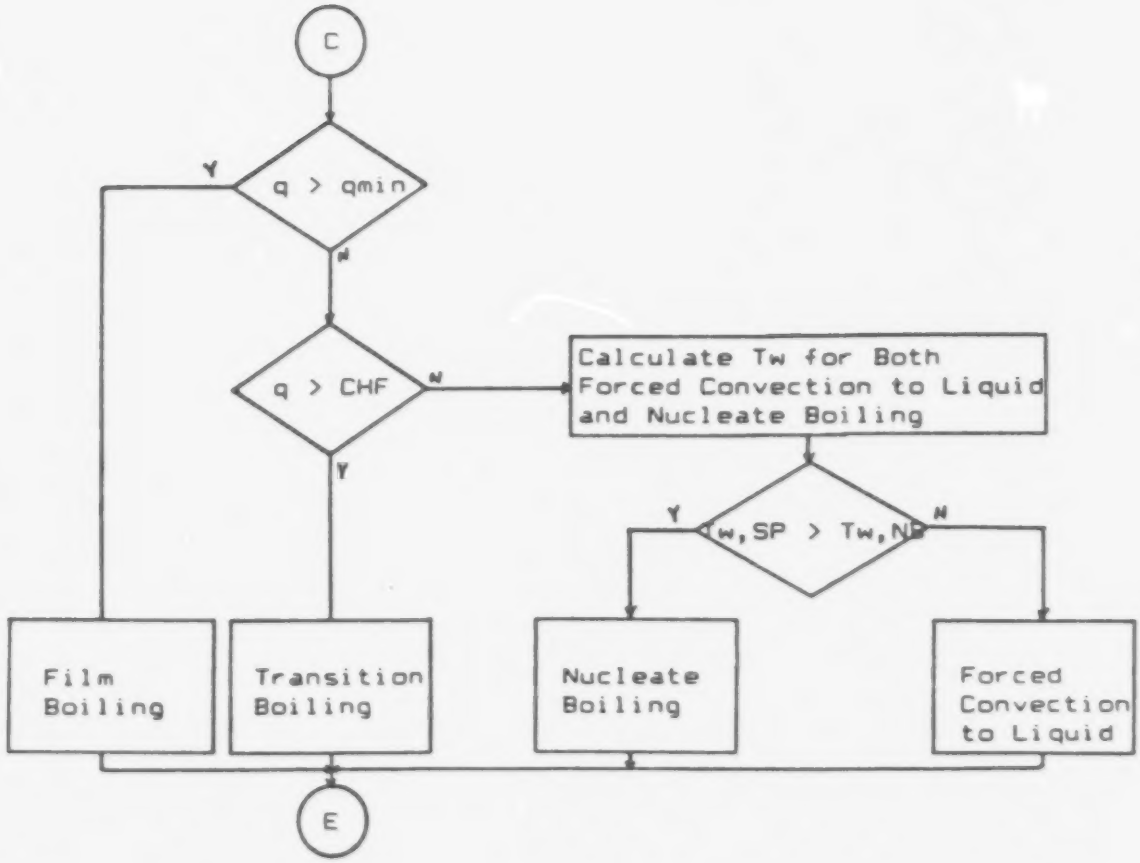

Figure 14. Heat Transfer Logic for a Heat Flux Controlled Mode (CHF < qmin)

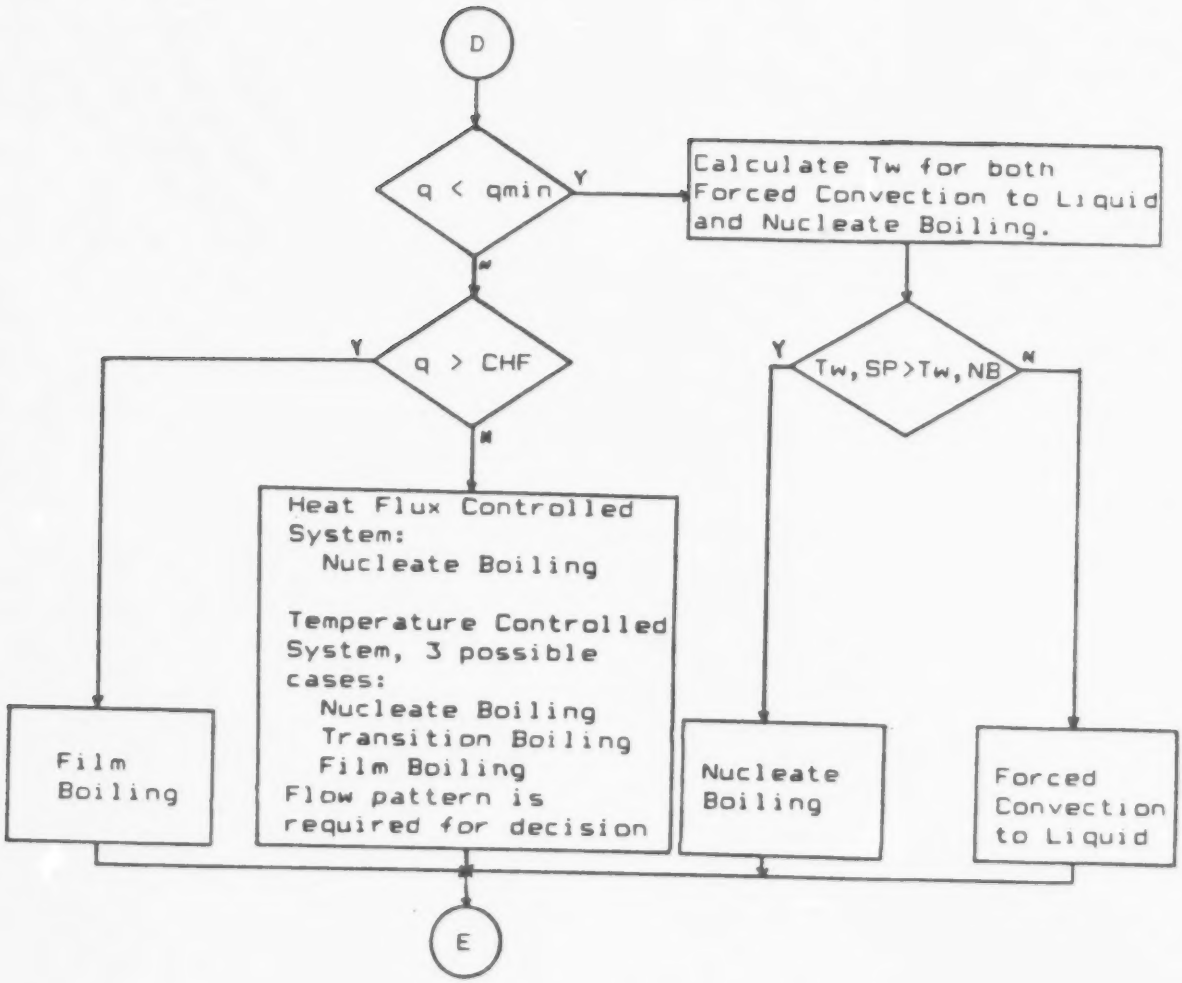

Figure 15. Heat Transfer Logic for a Heat Flux Controlled Mode (CHF > qmin)

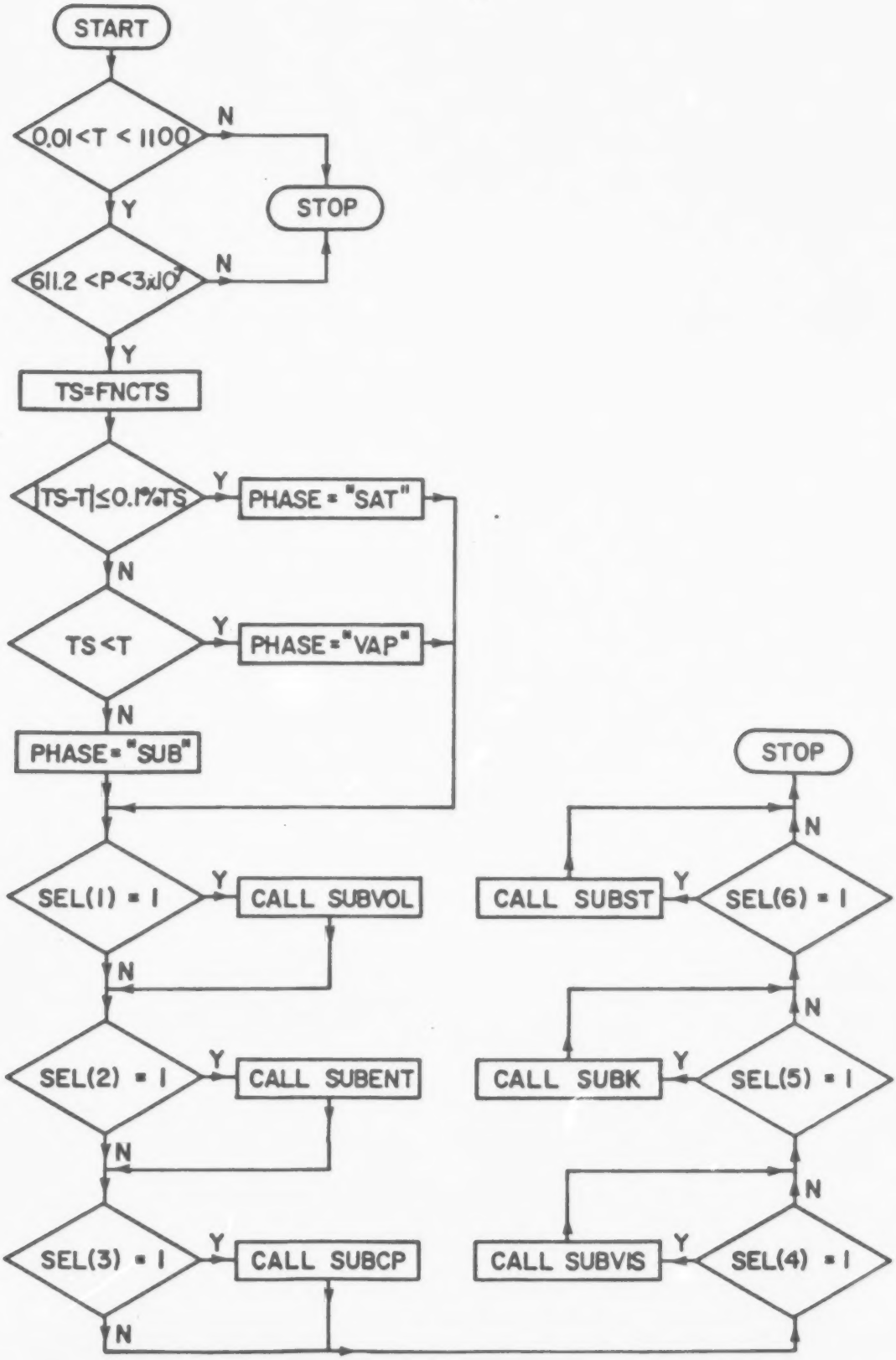

Figure 16(a) Flowchart for First Level

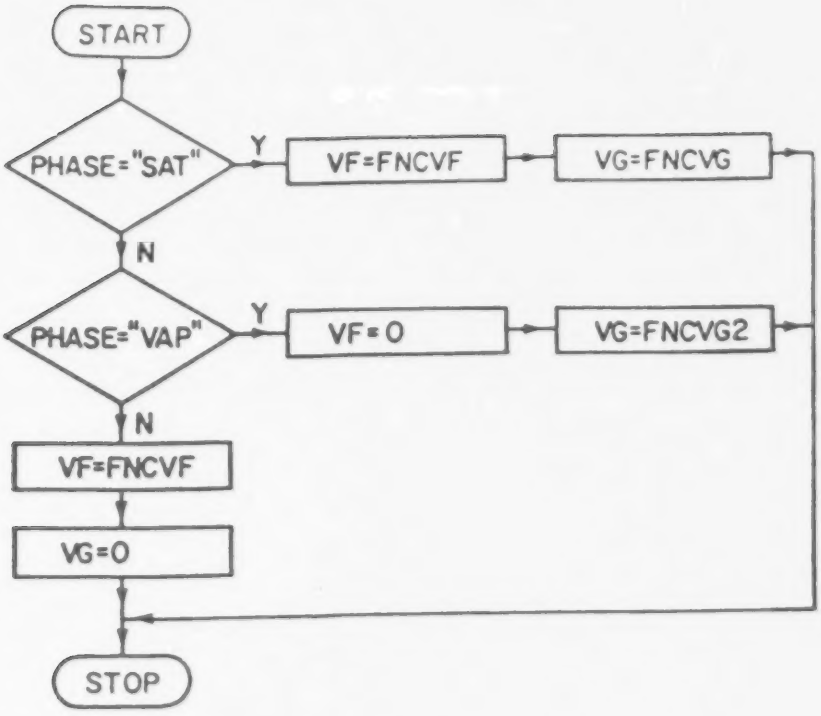

Figure 16(b). Flowchart for Second Level

```
Please enter choice of unit      :  S  <S> = SI    ; <B> = British
Please enter choice of geometry  :  T  <T> = tube  ; <B> = bundle
Please enter choice of fluid     :  H  <H> = H2O   ; <D> = D2O
Please enter channel orientation:  V  <H> = Hori.; <V> = Vert.
Please enter choice of state     :  S  <S> = Steady <T> = Transient
```

<ESC>=terminate; <Ctrl-End>=next page

Figure 17. Printout of the General Parameters Input Page

Pressure	P : 10000	kPa
Mass flux	G : 4000	kg/m²/s
Hydraulic diameter	D : 0.01	m
Quality	X : 0.2	
Heat flux	Q : 500	kW/m²

<ESC> = terminate; <Ctrl-End> = execute

Figure 18. Printout of the Steady State Parameters Input Page

Rod diameter	R :	0.01304	m
Hydraulic diameter	D :	0.0075862	m
Flow area	A :	0.00334	m^2

<ESC> = terminate; <Ctrl-End> = next page

Figure 19. Printout of the Time Indepedent Transient Parameters Input Page

Time sec	Pressure kPa	Mass Flux $kg/m^2/s$	Quality	Qgen kW/m3
0.	11400	7200	0.0212	366972
12.5	10800	6800	0.03	366972

<ESC> = terminate; <Ctrl-End> = execute

Figure 20. Printout of the Time Dependent Transient Parameters Input Page

```
Critical heat flux              CHF  :     1343.28 kW/m²
Critical heat flux temp.        TCHF :      319.65 °C
Min. film boiling temp.         TMIN :      382.31 °C
Min. film boiling heat flux     QMIN :      525.11 kW/m²

Heat transfer mode                   : NUCLEATE BOILING

Corresponding heat flux         Q    :      500.00 kW/m²

Corresponding wall temp.        TW   :      315.67 °C

Heat transfer coefficient       HTC  :      116.68 kW/m²°C

Next case? (Y/N)
```

Figure 21. Printout of the Steady State Output Page for Unique Heat Transfer Mode

```
Critical heat flux              CHF  :     1343.28 kW/m²
Critical heat flux temp.        TCHF :      319.65 °C
Min. film boiling temp.         TMIN :      382.31 °C
Min. film boiling heat flux     QMIN :      525.11 kW/m²

1:HEAT FLUX CONTROLLED;ALL:POSSIBLE FOR TEMP. CONTROLLED
Heat transfer mode                   : NUCLEATE BOILING
Corresponding heat flux         Q    :     1000.00 kW/m²
Corresponding wall temp.        TW   :      318.37 °C
Heat transfer coefficient       HTC  :      143.29 kW/m²°C
Heat transfer mode                   : TRANSITION BOILING
Corresponding heat flux         Q    :     1000.00 kW/m²
Corresponding wall temp.        TW   :      327.62 °C
Heat transfer coefficient       HTC  :       61.60 kW/m²°C
Heat transfer mode                   : FILM BOILING
Corresponding heat flux         Q    :     1000.00 kW/m²
Corresponding wall temp.        TW   :      525.56 °C
Heat transfer coefficient       HTC  :        4.83 kW/m²°C

Type <M> to modify, <I> to input, and <K> to keep the data
```

Figure 22. Printout of the Steady State Output Page for Multiple Heat Transfer Modes

Time sec	Pressure kPa	Mass Flux kg/m²/s	Quality	Qgen kW/m3	Twall °C	Qsur kW/m²
0.00	11400.00	7200.00	0.021200	366972.0	329.43	1196.3
12.50	10800.00	6800.00	0.030000	366972.0	325.40	1196.3

Enter any key to continue...

Figure 23. Printout of the Transient State Output Page

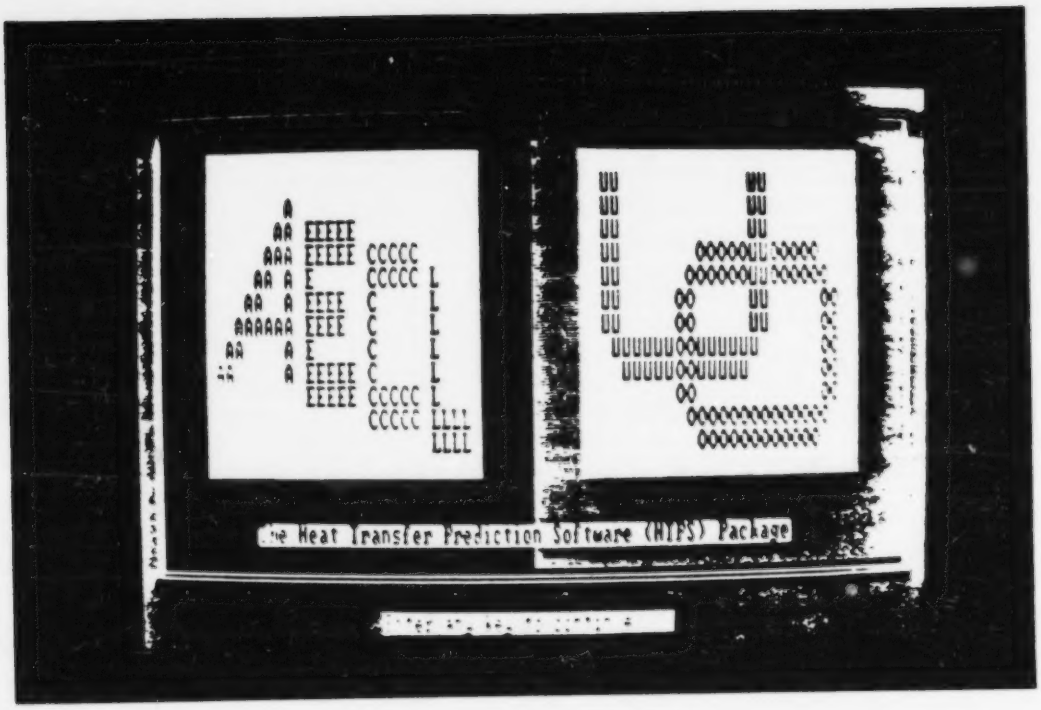

Figure 24. HTPS Logo Screen

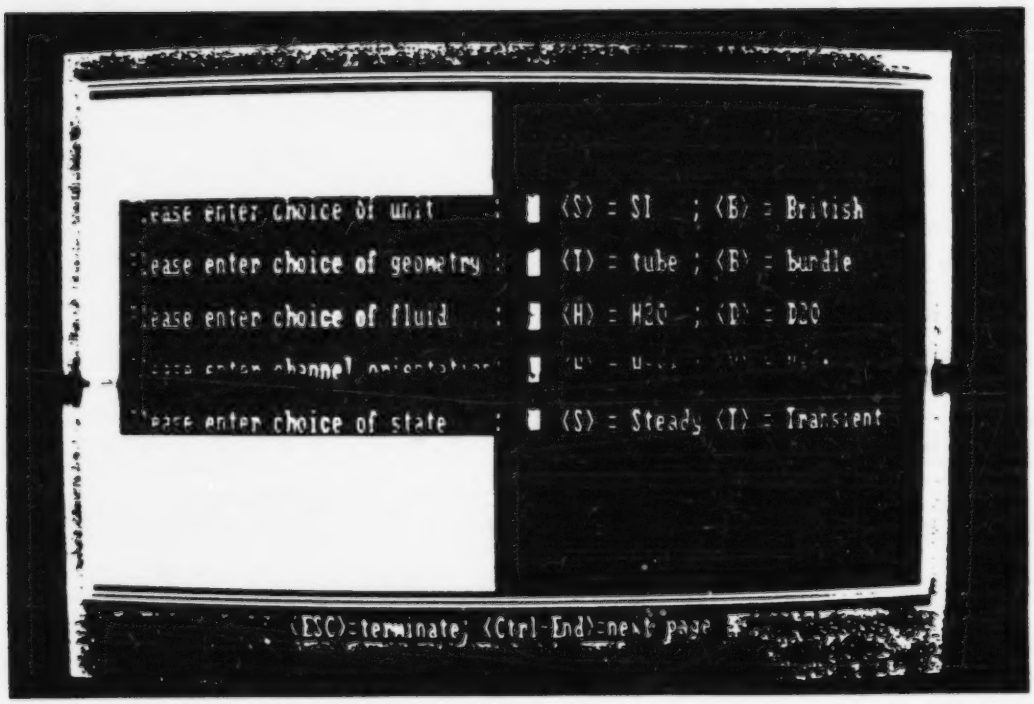
Please enter choice of unit : (S) = SI ; (B) = British
Please enter choice of geometry : (T) = tube ; (B) = bundle
Please enter choice of fluid : (H) = H2O ; (D) = D2O
Please enter choice of state : (S) = Steady (T) = Transient
(ESC)=terminate; (Ctrl-End)=next page

Figure 25. HTPS General Parameters Input Screen

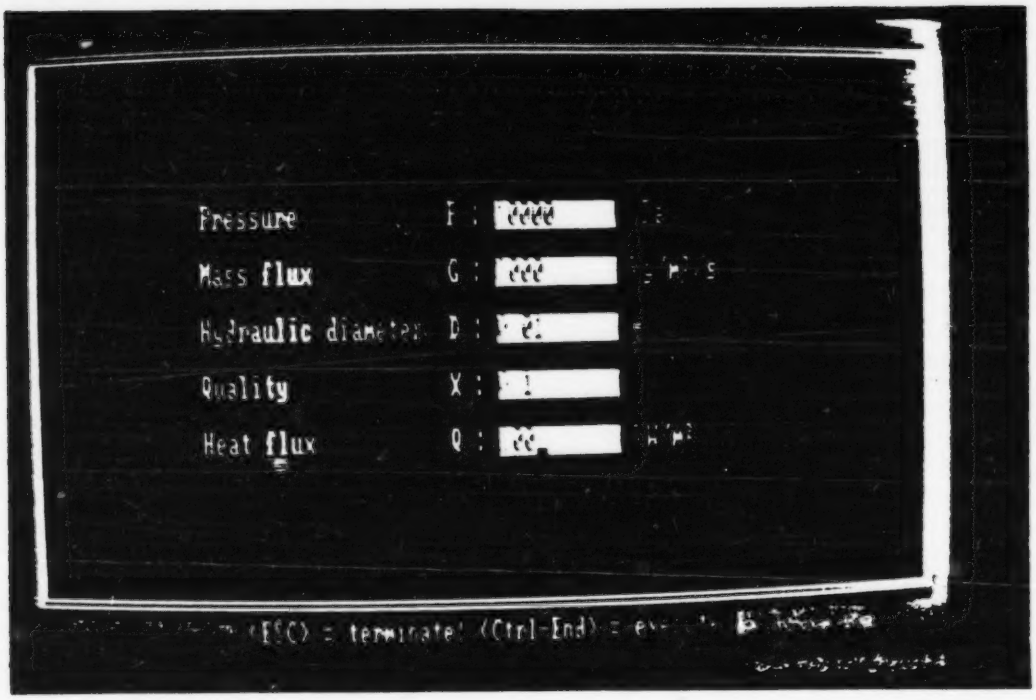

Figure 26. HTPS Steady State Parameters Input Screen

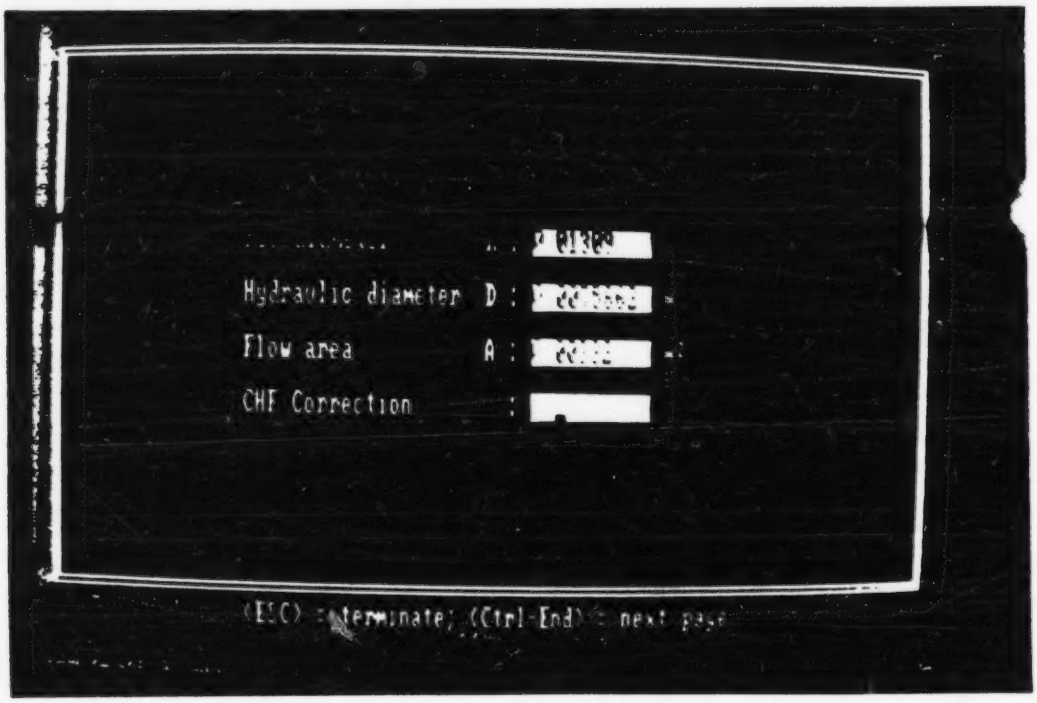

Figure 27. HTPS Transient State Time Indepedent Parameters Input Screen

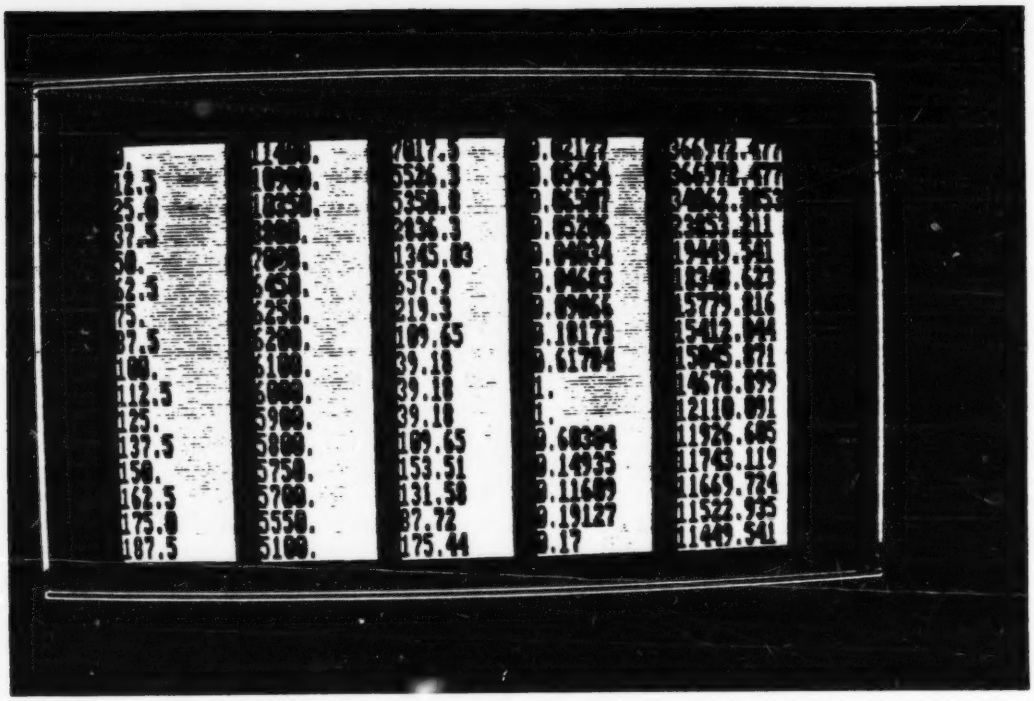

Figure 28. HTPS Transient State Time Depedent Parameters Input Screen

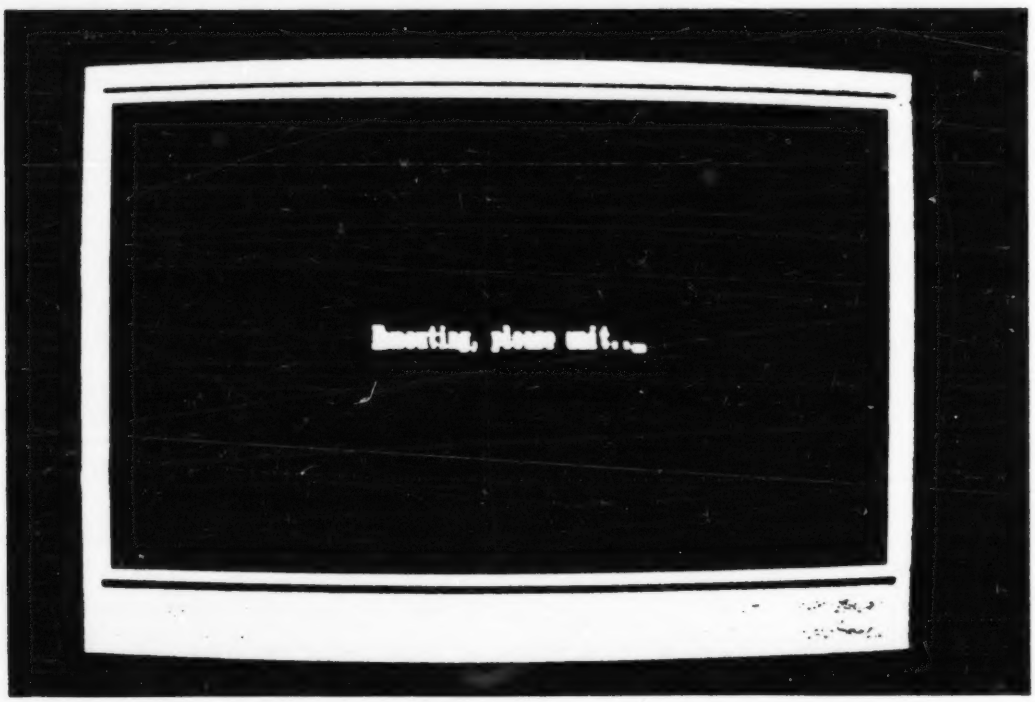

Figure 29. HTPS Execution Message Screen

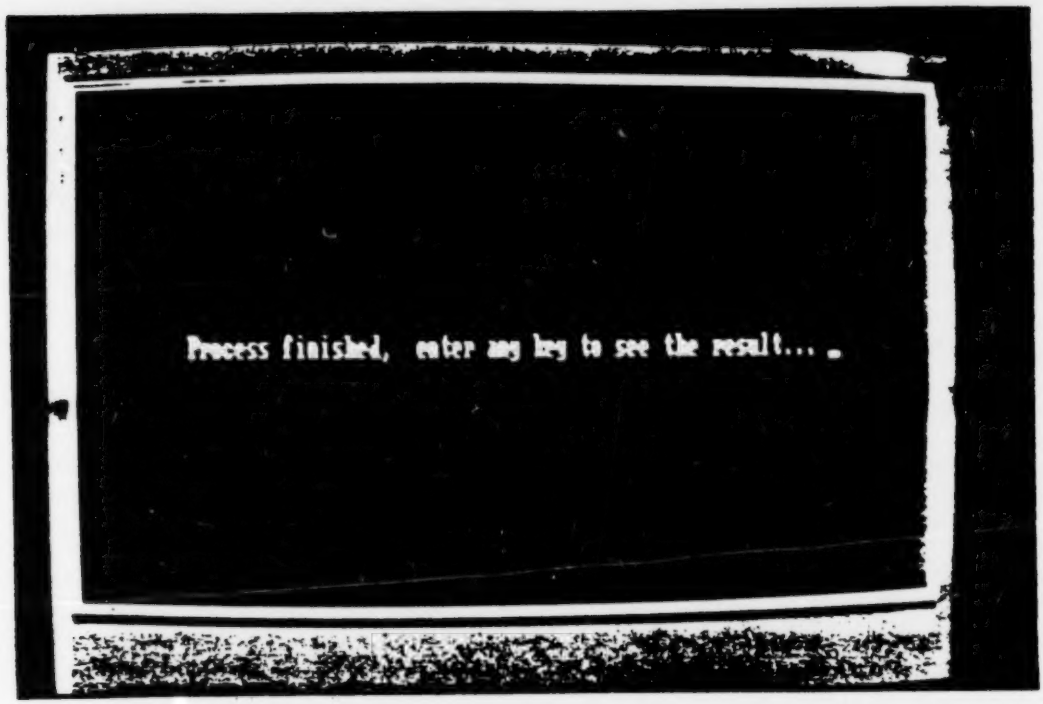

Figure 30. HTPS Finishing Message Screen

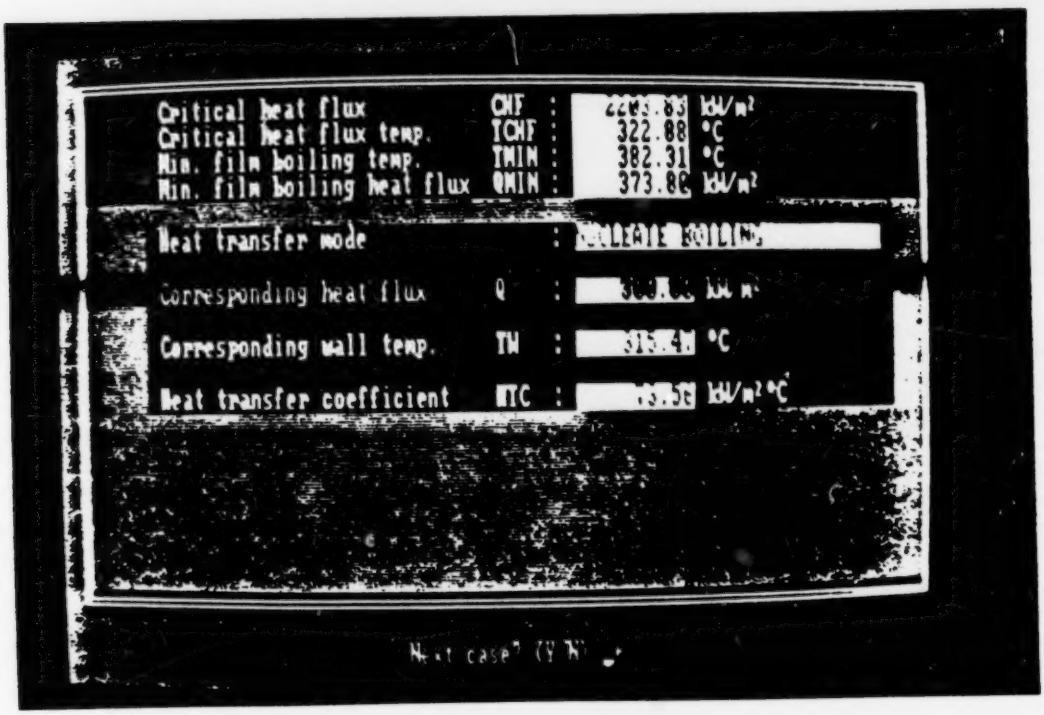
Critical heat flux CHF : kW/m²
Critical heat flux temp. TCHF : 322.88 °C
Min. film boiling temp. TMIN : 382.31 °C
Min. film boiling heat flux QMIN : 373.8 kW/m²
Heat transfer mode :
Corresponding heat flux Q :
Corresponding wall temp. TW : °C
Heat transfer coefficient HTC :

Figure 31. HTPS Steady State Output Screen for Unique Heat Transfer Mode

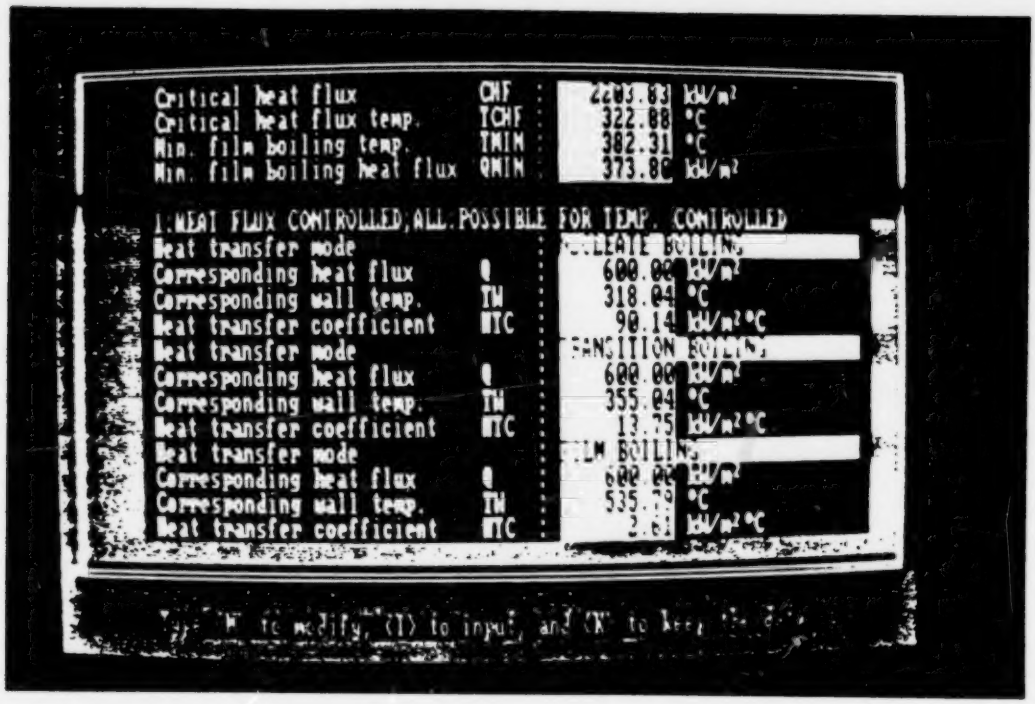
Critical heat flux CHF 2203.83 kW/m²
Critical heat flux temp. TCHF 322.88 °C
Min. film boiling temp. TMIN 382.31 °C
Min. film boiling heat flux QMIN 373.80 kW/m²
1:HEAT FLUX CONTROLLED;ALL POSSIBLE FOR TEMP. CONTROLLED
Heat transfer mode
Corresponding heat flux Q 600.00 kW/m²
Corresponding wall temp. TW 318.04 °C
Heat transfer coefficient HTC 90.14 kW/m²°C
Heat transfer mode
Corresponding heat flux Q 600.00 kW/m²
Corresponding wall temp. TW 355.04 °C
Heat transfer coefficient HTC 13.75 kW/m²°C
Heat transfer mode
Corresponding heat flux Q 600.00 kW/m²
Corresponding wall temp. TW 535.79 °C
Heat transfer coefficient HTC 2.61 kW/m²°C

Figure 32. HTPS Steady State Output Screen for Multiple Heat Transfer Modes

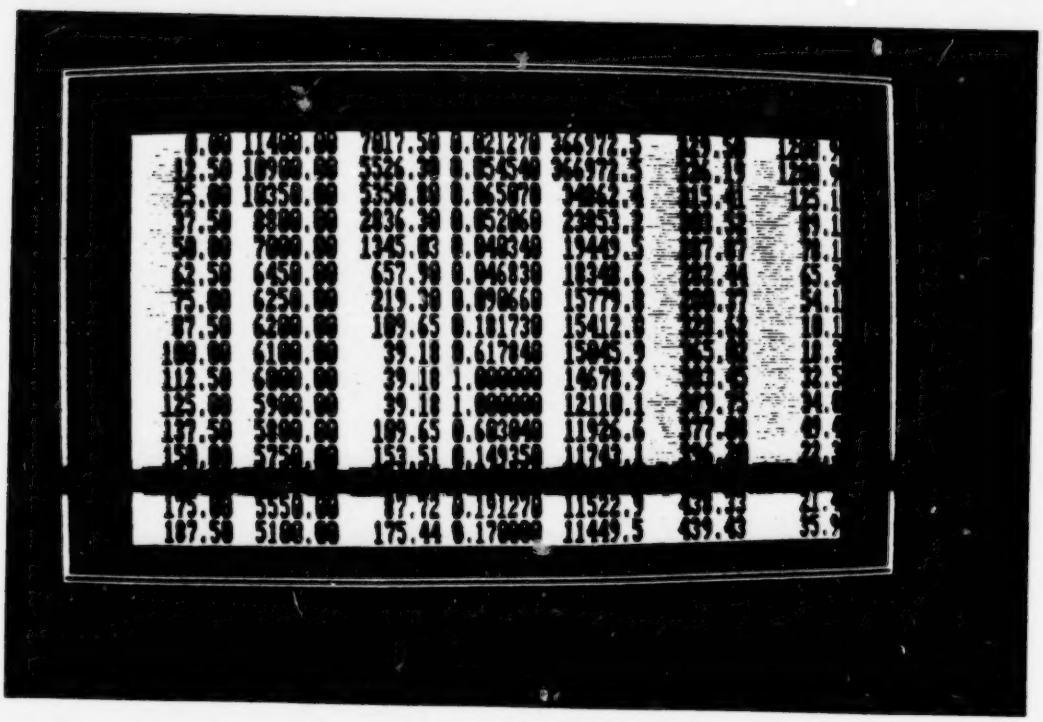

Figure 33. HTPS Transient State Output Screen